

PHASE PORTRAITS OF A FAMILY OF KOLMOGOROV SYSTEMS DEPENDING ON SIX PARAMETERS

ÉRIKA DIZ-PITA, JAUME LLIBRE, M. VICTORIA OTERO-ESPINAR

ABSTRACT. We consider a general 3-dimensional Lotka-Volterra system with a rational first integral of degree two of the form $H = x^i y^j z^k$. The restriction of this Lotka-Volterra system to each surface $H(x, y, z) = h$ varying $h \in \mathbb{R}$ provide Kolmogorov systems. With the additional assumption that they have a Darboux invariant of the form $x^\ell y^m e^{st}$ they reduce to the Kolmogorov systems

$$\begin{aligned}\dot{x} &= x(a_0 - \mu(c_1 x + c_2 z^2 + c_3 z)), \\ \dot{z} &= z(c_0 + c_1 x + c_2 z^2 + c_3 z).\end{aligned}$$

We classify the phase portraits in the Poincaré disc of all these Kolmogorov systems which depend on six parameters.

1. INTRODUCTION

The Lotka-Volterra systems have been used for modeling many natural phenomena, such as the time evolution of conflicting species in biology [20], chemical reactions, plasma physics [15] or hydrodynamics [6], just as other problems from social science and economics.

These systems, which are polynomial differential equations of degree two, were initially proposed, independently, by Lotka in 1925 and Volterra in 1926, both in the context of competing species. Later on Lotka-Volterra systems were generalized and considered in arbitrary dimension, i.e.

$$\dot{x}_i = x_i \left(a_{i0} + \sum_{j=1}^n a_{ij} x_j \right), \quad i = 1, \dots, n.$$

Consequently the applications of these systems started to multiply. Moreover Kolmogorov in [14] extended the Lotka-Volterra systems as follows

$$\dot{x}_i = x_i P_i(x_1, \dots, x_n), \quad i = 1, \dots, n,$$

where P_i are polynomials of degree at most m . These kind of systems are now known as Kolmogorov systems. They have in particular all the applications of the Lotka-Volterra systems as for instance in the study of the black holes in cosmology, see [1].

2010 *Mathematics Subject Classification.* 34C05.

Key words and phrases. Kolmogorov system; Lotka-Volterra system; phase portrait; Poincaré disc.

©2021 Texas State University.

Submitted June 1, 2020. Published May 3, 2021.

The global qualitative dynamics of the Lotka-Volterra systems in dimension two has been completely studied in [24], where all possible phase portraits on the Poincaré disc have been classified.

There are few results about the global dynamics of the Lotka-Volterra systems in dimension three. Our objective is to study the phase portraits of the 3-dimensional Lotka-Volterra systems

$$\begin{aligned}\dot{x} &= x(a_0 + a_1x + a_2y + a_3z), \\ \dot{y} &= y(b_0 + b_1x + b_2y + b_3z), \\ \dot{z} &= z(c_0 + c_1x + c_2y + c_3z),\end{aligned}\tag{1.1}$$

which have a rational first integral of degree two of the form $x^i y^j z^k$. We have used the Darboux theory of integrability to obtain a characterization of these systems. As a result, we have reduced the initial problem to a problem in dimension two, the study of the global dynamics of two families of Kolmogorov systems. In this paper we focus on the first family, which is

$$\begin{aligned}\dot{x} &= x(a_0 + a_1x + a_2z^2 + a_3z), \\ \dot{z} &= z(c_0 + c_1x + c_2z^2 + c_3z),\end{aligned}\tag{1.2}$$

Kolmogorov systems (1.2) depend on eight parameters, this is a big number to classify all their distinct topological phase portraits. Then we require that Kolmogorov systems (1.2) have a Darboux invariant of the form $x^\ell y^m e^{st}$, then these systems are reduced to study the Kolmogorov systems

$$\begin{aligned}\dot{x} &= x(a_0 - \mu(c_1x + c_2z^2 + c_3z)), \\ \dot{z} &= z(c_0 + c_1x + c_2z^2 + c_3z),\end{aligned}\tag{1.3}$$

which now depend on six parameters. For these Kolmogorov systems we give the topological classification of all their phase portraits in the Poincaré disc. Roughly speaking the Poincaré disc is the closed unit disc centered at the origin of \mathbb{R}^2 . Its interior is identified with \mathbb{R}^2 and the circle of its boundary is identified with the infinity of \mathbb{R}^2 . In the plane \mathbb{R}^2 we can go or come from the infinity in as many directions as points have the circle. The polynomial differential systems can be extended to the closed Poincaré disc, i.e. they can be extended to infinity and in this way we can study their dynamics in a neighborhood of infinity. This extension is called the Poincaré compactification, for more details see subsection 2.1. Thus our main result is the following.

Theorem 1.1. *Kolmogorov systems (1.3) have 102 topologically distinct phase portraits in the Poincaré disc under condition (H1) given in Figure 16.*

$$(H1) \quad c_2 \neq 0, a_0 \geq 0, c_1 \geq 0, c_3 \geq 0, a_0 + c_0\mu \neq 0, a_0c_1\mu \neq 0, \mu \neq -1$$

We will see that we can assume condition (H1) because Kolmogorov systems (1.3) can be reduced to satisfy such condition either using symmetries, or eliminating known phase portraits, or eliminating phase portraits with infinitely many finite or infinite singular points. Some topological phase portraits have been classified in the Poincaré disc are; see for instance [4, 13, 17].

In Section 3 using the Darboux theory of integrability we explain the reduction from the Lotka-Volterra system (1.1) to the Kolmogorov systems (1.3). In Section 4 we give some properties of the system obtained. In Section 5 we study the local phase portrait of the finite singular points, and in Section 6 we do the same with

the infinite singular points, applying the blow-up technique. Finally in Section 7 we prove Theorem 1.1.

2. PRELIMINARIES

2.1. Poincaré compactification. To study the behavior of the trajectories of our polynomial differential systems near infinity we will use the Poincaré compactification. We provide a short summary about this method, more details can be found in [9, Chapter 5].

Let $X = (P(x, y), Q(x, y))$ be a polynomial vector field of degree d defined in \mathbb{R}^2 . Consider the *Poincaré sphere* $\mathbb{S}^2 = \{y \in \mathbb{R}^3 : y_1^2 + y_2^2 + y_3^2 = 1\}$, and its tangent plane at the point $(0, 0, 1)$ which is identified with \mathbb{R}^2 .

We consider the central projections $f^+ : \mathbb{R}^2 \rightarrow \mathbb{S}^2$ and $f^- : \mathbb{R}^2 \rightarrow \mathbb{S}^2$. By definition, $f^+(x)$ is the intersection of the straight line passing through the point x and the origin with the northern hemisphere of \mathbb{S}^2 , and respectively for $f^-(x)$ with the southern hemisphere. The differential Df^+ and respectively Df^- send the vector field X into a vector field \bar{X} on $\mathbb{S}^2 \setminus \mathbb{S}^1$. Note that the points at infinity of \mathbb{R}^2 are in bijective correspondence with the points of the equator \mathbb{S}^1 of \mathbb{S}^2 .

The vector field \bar{X} can be extended analytically to a vector field on \mathbb{S}^2 multiplying \bar{X} by y_3^d . We denote this vector field by $\rho(X)$, and it is called the *Poincaré compactification* of the vector field X on \mathbb{R}^2 .

For studying the dynamics of X in the neighborhood of the infinity, we must study the dynamics of $\rho(X)$ near \mathbb{S}^1 . The sphere \mathbb{S}^2 is a 2-dimensional manifold so we need to know the expressions of the vector field $\rho(X)$ in the local charts (U_i, ϕ_i) and (V_i, ψ_i) , where $U_i = \{y \in \mathbb{S}^2 : y_i > 0\}$, $V_i = \{y \in \mathbb{S}^2 : y_i < 0\}$, $\phi_i : U_i \rightarrow \mathbb{R}^2$ and $\psi_i : V_i \rightarrow \mathbb{R}^2$ for $i = 1, 2, 3$ with $\phi_i(y) = -\psi_i(y) = (y_m/y_i, y_n/y_i)$ for $m < n$ and $m, n \neq i$.

In the local chart (U_1, ϕ_1) the expression of $\rho(X)$ is

$$\dot{u} = v^d \left[-uP\left(\frac{1}{v}, \frac{u}{v}\right) + Q\left(\frac{1}{v}, \frac{u}{v}\right) \right], \quad \dot{v} = -v^{d+1}P\left(\frac{1}{v}, \frac{u}{v}\right). \quad (2.1)$$

In the local chart (U_2, ϕ_2) the expression of $\rho(X)$ is

$$\dot{u} = v^d \left[P\left(\frac{1}{v}, \frac{u}{v}\right) - uQ\left(\frac{1}{v}, \frac{u}{v}\right) \right], \quad \dot{v} = -v^{d+1}P\left(\frac{1}{v}, \frac{u}{v}\right), \quad (2.2)$$

and in the local chart (U_3, ϕ_3) the expression of $\rho(X)$ is

$$\dot{u} = P(u, v), \quad \dot{v} = Q(u, v). \quad (2.3)$$

In the charts (V_i, ψ_i) , with $i = 1, 2, 3$, the expression for $\rho(X)$ is the same as in the charts (U_i, ϕ_i) multiplied by $(-1)^{d-1}$.

The equator \mathbb{S}^1 is invariant by the vector field $\rho(X)$ and all the singular points of $\rho(X)$ which lie in this equator are called the *infinite singular points* of X . If $y \in \mathbb{S}^1$ is an infinite singular point, then $-y$ is also an infinite singular point and they have the same (respectively opposite) stability if the degree of vector field is odd (respectively even).

The image of the closed northern hemisphere of \mathbb{S}^2 onto the plane $y_3 = 0$ under the orthogonal projection π is called the *Poincaré disc* \mathbb{D}^2 . Since the orbits of $\rho(X)$ on \mathbb{S}^2 are symmetric with respect to the origin of \mathbb{R}^3 , we only need to consider the flow of $\rho(X)$ in the closed northern hemisphere, and we can project the phase portrait of $\rho(X)$ on the northern hemisphere onto the Poincaré disc. We shall present the phase portraits of the polynomial differential systems (1.3) in the Poincaré disc.

2.2. Topological equivalence between two polynomial vector fields. Two polynomial vector fields X_1 and X_2 on \mathbb{R}^2 are *topologically equivalent* if there exists a homeomorphism on the Poincaré disc which preserves the infinity \mathbb{S}^1 and sends the trajectories of the flow of $\pi(\rho(X_1))$ to the trajectories of the flow of $\pi(\rho(X_2))$, preserving or reversing the orientation of all the orbits.

A *separatrix* of the Poincaré compactification $\pi(\rho(X))$ is an orbit at the infinity \mathbb{S}^1 , or a finite singular point, or a limit cycle, or an orbit on the boundary of a hyperbolic sector at a finite or an infinite singular point. The set of all separatrices of $\pi(\rho(X))$ is closed and we denote it by Σ_X .

An open connected component of $\mathbb{D}^2 \setminus \Sigma_X$ is a *canonical region* of $\pi(\rho(X))$. The *separatrix configuration* of $\pi(\rho(X))$ is the union of an orbit of each canonical region with the set Σ_X , and it is denoted by Σ'_X . We denote by S (respectively R) the number of separatrices (respectively canonical regions) of a vector field $\pi(\rho(X))$.

We say that two separatrix configurations Σ'_{X_1} and Σ'_{X_2} are *topologically equivalent* if there is a homeomorphism $h : \mathbb{D}^2 \rightarrow \mathbb{D}^2$ such that $h(\Sigma'_{X_1}) = \Sigma'_{X_2}$.

The following theorem of Markus [21], Neumann [22] and Peixoto [23] allows us to investigate only the separatrix configuration of a polynomial differential system in order to determine its phase portrait in the Poincaré disc.

Theorem 2.1. *The phase portraits in the Poincaré disc of two compactified polynomial vector fields $\pi(\rho(X_1))$ and $\pi(\rho(X_2))$ with finitely many separatrices are topologically equivalent if and only if their separatrix configurations Σ'_{X_1} and Σ'_{X_2} are topologically equivalent.*

2.3. Blow-up technique. There exist classification theorems for hyperbolic and semi-hyperbolic singular points, and also for nilpotent singular points which can be found in [9, Chapter 2]. The centers are more difficult to study, see for instance [9, Chapter 4]. Whereas to study a singular point for which the Jacobian matrix is identically zero, the only possibility is studying each singular point case by case. The main technique to perform the desingularization of a linearly zero singular point is the blow-up technique. We give a short summary about this method, more details can be found in [2].

Roughly speaking the idea behind the blow up technique is to explode, through a change of variables that is not a diffeomorphism, the singularity to a line. Then, for studying the original singular point, one studies the new singular points that appear on this line, and this is simpler. If some of these new singular points are linearly zero, the process is repeated. Dumortier proved that this iterative process of desingularization is finite, see [8].

Consider a real planar polynomial differential system

$$\begin{aligned} \dot{x} &= P(x, y) = P_m(x, y) + \dots, \\ \dot{y} &= Q(x, y) = Q_m(x, y) + \dots, \end{aligned} \tag{2.4}$$

where P and Q are coprime polynomials, P_m and Q_m are homogeneous polynomials of degree $m \in \mathbb{N}$ and the dots mean higher order terms in x and y . Note that we are assuming that the origin is a singular point because $m > 0$. We define the *characteristic polynomial* of (2.4) as

$$\mathcal{F}(x, y) := xQ_m(x, y) - yP_m(x, y), \tag{2.5}$$

and we say that the origin is a *nondicritical* singular point if $\mathcal{F} \neq 0$ and a *dicritical* singular point if $\mathcal{F} \equiv 0$. In this last case $P_m = xW_{m-1}$ and $Q_m = yW_{m-1}$, where

$W_{m-1} \neq 0$ is a homogeneous polynomial of degree $m - 1$. If $y - vx$ is a factor of W_{m-1} and $v = \tan \theta^*$, $\theta^* \in [0, 2\pi)$, then θ^* is a *singular direction*.

The *homogeneous directional blow up in the vertical direction* is the mapping $(x, y) \rightarrow (x, z) = (x, y/x)$, where z is a new variable. This map transforms the origin of (2.4) into the line $x = 0$, which is called the *exceptional divisor*. The expression of system (2.4) after the blow up in the vertical direction is

$$\dot{x} = P(x, xz), \quad \dot{z} = \frac{Q(x, xz) - zP(x, xz)}{x}, \quad (2.6)$$

that is always well-defined since we are assuming that the origin is a singularity. After the blow up, we cancel an appearing common factor x^{m-1} (x^m if $\mathcal{F} \equiv 0$). Moreover, the mapping swaps the second and the third quadrants in the vertical directional blow up. [2, Propositions 2.1 and 2.2] provide the relationship between the original singular point of system (2.4) and the new singularities of system (2.6). For additional details see [3].

Finally, to study the behavior of the solutions around the origin of system (2.4), it is necessary to study the singular points of system (2.6) on the exceptional divisor. They correspond to either characteristic directions in the nondicritical case, or singular directions in the dicritical case. It may happen that some of these singular points are linearly zero, in which case we have to repeat the process. As we said before, it is proved in [8] that this chain of blow ups is finite.

2.4. Indices of planar singular points. Given an isolated singularity q of a vector field X , defined on an open subset of \mathbb{R}^2 or \mathbb{S}^2 , we define the index of q by means of the Poincaré Index Formula. We assume that q has the finite sectorial decomposition property. Let e , h and p denote the number of elliptic, hyperbolic and parabolic sectors of q , respectively, and suppose that $e + h + p > 0$. Then the *index of q* is $i_q = 1 + (e - h)/2$, and it is always an integer.

We recall that the Poincaré compactification of a vector field in \mathbb{R}^2 introduced in Subsection 2.1 is a tangent vector field on the sphere \mathbb{S}^2 , so the next result will be very useful in our study.

Theorem 2.2 (Poincaré-Hopf Theorem). *For every tangent vector field on \mathbb{S}^2 with a finite number of singular points, the sum of their indices is 2.*

2.5. Invariants and Application of the Darboux Theory. The Darboux Theory of Integrability provides a link between the integrability of polynomial vector fields and the number of invariant algebraic curves that they have. The basic results on dimension two can be found in Chapter 8 of [9], and these results have been extended to \mathbb{R}^n and \mathbb{C}^n in [16, 18, 19].

We consider a real polynomial differential system in dimension three, that is a system of the form

$$\begin{aligned} dx/dt &= \dot{x} = P(x, y, z), \\ dy/dt &= \dot{y} = Q(x, y, z), \\ dz/dt &= \dot{z} = R(x, y, z), \end{aligned} \quad (2.7)$$

where P, Q and R are polynomials in the variables x, y and z . We denote by $m = \max\{\deg P, \deg Q, \deg R\}$ the degree of the polynomial system, and we always assume that the polynomials P, Q and R are relatively prime in the ring of the real polynomials in the variables x, y and z .

Theorem 2.3 (Darboux Integrability Theorem). *Suppose that a polynomial system (2.7) of degree m admits p irreducible invariant algebraic surfaces $f_i = 0$ with cofactors K_i for $i = 1, \dots, p$. Then the next statements hold.*

- (a) *There exist $\lambda_i \in \mathbb{C}$ not all zero such that $\sum_{i=1}^p \lambda_i K_i = 0$ if and only if the function $f_1^{\lambda_1} \dots f_p^{\lambda_p}$ is a first integral of system (2.7).*
- (b) *There exist $\lambda_i \in \mathbb{C}$ not all zero such that $\sum_{i=1}^p \lambda_i K_i = -s$ for some $s \in \mathbb{R} \setminus \{0\}$ if and only if the function $f_1^{\lambda_1} \dots f_p^{\lambda_p} \exp(st)$ is a Darboux invariant of system (2.7).*

3. REDUCTION OF THE LOTKA-VOLTERRA SYSTEMS IN \mathbb{R}^3 TO THE KOLMOGOROV SYSTEMS IN \mathbb{R}^2

As we said our objective is to study the global dynamics of the Lotka-Volterra systems (1.1) in dimension three, which have a rational first integral of degree two of the form $x^i y^j z^k$. The Darboux theory of integrability allow us to obtain a characterization of these systems.

We consider the irreducible invariant algebraic surfaces $f_1(x, y, z) = x = 0$, $f_2(x, y, z) = y = 0$ and $f_3(x, y, z) = z = 0$ of system (1.1), with cofactors K_1 , K_2 and K_3 , respectively. As K_i is the cofactor of f_i we have that

$$Xf_i = P \frac{\partial f_i}{\partial x} + Q \frac{\partial f_i}{\partial y} + R \frac{\partial f_i}{\partial z} = K_i f_i.$$

Then for the invariant algebraic surfaces considered we obtain the cofactors $K_1 = a_0 + a_1 x + a_2 y + a_3 z$, $K_2 = b_0 + b_1 x + b_2 y + b_3 z$, and $K_3 = c_0 + c_1 x + c_2 y + c_3 z$, respectively.

Applying Theorem 2.3, since we assume that $x^{\lambda_1} y^{\lambda_2} z^{\lambda_3}$ is a first integral of system (1.1), we obtain that there exist $\lambda_i \in \mathbb{C}$, with $i \in \{1, 2, 3\}$, not all zero, such that $\sum_{i=1}^3 \lambda_i K_i = 0$. Apart from the trivial solution $\{\lambda_1 = 0, \lambda_2 = 0, \lambda_3 = 0\}$, there are the following three solutions of this equation:

$$\begin{aligned} S_1 &= \{c_0 = 0, c_1 = 0, c_2 = 0, c_3 = 0, \lambda_2 = 0, \lambda_1 = 0\}, \\ S_2 &= \{b_0 = -\frac{c_0 \lambda_3}{\lambda_2}, b_1 = -\frac{c_1 \lambda_3}{\lambda_2}, b_2 = -\frac{c_2 \lambda_3}{\lambda_2}, b_3 = -\frac{c_3 \lambda_3}{\lambda_2}, \lambda_1 = 0\}, \\ S_3 &= \{a_0 = \frac{-b_0 \lambda_2 - c_0 \lambda_3}{\lambda_1}, a_1 = \frac{-b_1 \lambda_2 - c_1 \lambda_3}{\lambda_1}, a_2 = \frac{-b_2 \lambda_2 - c_2 \lambda_3}{\lambda_1}, \\ & a_3 = \frac{-b_3 \lambda_2 - c_3 \lambda_3}{\lambda_1}\}, \end{aligned}$$

which give rise to three families of Lotka-Volterra polynomial differential systems of degree two in \mathbb{R}^3 , with a first integral of the form $x^{\lambda_1} y^{\lambda_2} z^{\lambda_3}$.

If we consider the family given by solution S_1 , as the parameters c_i , $i = 0, \dots, 3$, are zero, we have that $\dot{z} = 0$ and the Lotka-Volterra system is reduced to:

$$\begin{aligned} \dot{x} &= x(a_0 + a_1 x + a_2 y + a_3 z), \\ \dot{y} &= y(b_0 + b_1 x + b_2 y + b_3 z), \\ \dot{z} &= 0. \end{aligned}$$

As $\dot{z} = 0$, z is constant and this system has $H = z$ as a first integral. Note that if we consider the first integral $H = x^{\lambda_1} y^{\lambda_2} z^{\lambda_3}$, and apply the conditions given by S_1 , it is $\lambda_1 = \lambda_2 = 0$, we obtain $H = z^{\lambda_3}$, with $\lambda_3 = 2$ for getting the degree two, but in this case we will consider the simplest first integral. In each invariant plane with z

constant, we have a Lotka-Volterra polynomial differential system in \mathbb{R}^2 . The phase portrait of these systems has been studied in [24], so we are not going to deal with this case.

In this article we study the family given by the solution S_2 . This solution provides the values of parameters b_i as a function of the parameters λ_2 , λ_3 and c_i , with $i = 0, \dots, 3$, so we can replace them in the expression of \dot{y} obtaining

$$\dot{y} = y \left(-\frac{c_0\lambda_3}{\lambda_2} - \frac{c_1\lambda_3}{\lambda_2}x - \frac{c_2\lambda_3}{\lambda_2}y - \frac{c_3\lambda_3}{\lambda_2}z \right).$$

If we denote $\lambda = -\lambda_3/\lambda_2$, then the original Lotka-Volterra system becomes

$$\begin{aligned}\dot{x} &= x(a_0 + a_1x + a_2y + a_3z), \\ \dot{y} &= \lambda y(c_0 + c_1x + c_2y + c_3z), \\ \dot{z} &= z(c_0 + c_1x + c_2y + c_3z).\end{aligned}$$

Given that $\lambda_1 = 0$, the first integral $H = x^{\lambda_1}y^{\lambda_2}z^{\lambda_3}$ is reduced to $H = y^{\lambda_2}z^{\lambda_3}$, but if this is a first integral, also $H = (y^{\lambda_2}z^{\lambda_3})^{-1/\lambda_2} = y^{-1}z^{-\lambda_3/\lambda_2} = y^{-1}z^\lambda = z^\lambda/y$ is a first integral. If we want H to be rational of degree two, we must take $\lambda = 2$. In each level $H = 1/h$, with $h \neq 0$, we will have $1/h = z^2/y$, so $y = hz^2$ and then, for each h , the initial Lotka-Volterra system on dimension three reduces to the system on dimension two

$$\begin{aligned}\dot{x} &= x(a_0 + a_1x + a_2hz^2 + a_3z), \\ \dot{z} &= z(c_0 + c_1x + c_2hz^2 + c_3z).\end{aligned}$$

We must study the phase portrait of the systems of this family, but it is equivalent to study the phase portraits of the family of Kolmogorov systems in dimension two

$$\begin{aligned}\dot{x} &= x(a_0 + a_1x + a_2z^2 + a_3z), \\ \dot{z} &= z(c_0 + c_1x + c_2z^2 + c_3z).\end{aligned}\tag{3.1}$$

In the particular cases in which H is zero or infinity, the differential system on dimension three is reduced to a Lotka-Volterra system on dimension two, having in each case $z = 0$ and $y = 0$, respectively. We recall that these systems had already been studied in [24].

Systems (3.1) depend on eight parameters and the classification of all their distinct topological phase portraits is huge. For this reason we study the subclass of them having a Darboux invariant of the form $x^{\lambda_1}z^{\lambda_2}e^{st}$. By statement (b) of Theorem 2.3 the expression $\lambda_1K_x + \lambda_2K_z + s$ must be zero, where K_x and K_y are the cofactors of the invariant planes $x = 0$ and $z = 0$, respectively. Note that s and $\lambda_1^2 + \lambda_2^2$ cannot be zero. We obtain the cofactors $K_x = a_0 + a_1x + a_2z^2 + a_3z$ and $K_z = c_0 + c_1x + c_2z^2 + c_3z$ and then, solving the equation $\lambda_1K_x + \lambda_2K_z + s = 0$, we obtain the following two non-trivial solutions

$$\begin{aligned}\tilde{S}_1 &= \left\{ s = -a_0\lambda_1 - c_0\lambda_2, a_1 = -\frac{c_1\lambda_2}{\lambda_1}, a_2 = -\frac{c_2\lambda_2}{\lambda_1}, a_3 = -\frac{c_3\lambda_2}{\lambda_1} \right\}, \\ \tilde{S}_2 &= \{ s = -c_0\lambda_2, c_1 = 0, c_2 = 0, c_3 = 0, \lambda_1 = 0 \}.\end{aligned}$$

So we have two subsystems from the initial system (3.1). According to the conditions given by solution \tilde{S}_1 the first subsystem is

$$\dot{x} = x \left(a_0 - \frac{c_1\lambda_2}{\lambda_1}x - \frac{c_2\lambda_2}{\lambda_1}z^2 - \frac{c_3\lambda_2}{\lambda_1}z \right),$$

$$\dot{z} = z(c_0 + c_1x + c_2z^2 + c_3z).$$

If we denote $\lambda_2/\lambda_1 = \mu$ and $\lambda_1 = \lambda$, then this subsystem becomes

$$\begin{aligned} \dot{x} &= x(a_0 - \mu(c_1x + c_2z^2 + c_3z)), \\ \dot{z} &= z(c_0 + c_1x + c_2z^2 + c_3z), \end{aligned} \quad (3.2)$$

and its Darboux invariant is $x^\lambda z^{\lambda\mu} e^{-t\lambda(a_0+c_0\mu)}$. But if this is a Darboux invariant, also it is $xz^\mu e^{-t(a_0+c_0\mu)}$. Note that in order that we have a Darboux invariant $a_0 + c_0\mu$ cannot be zero.

If we consider now the solution \tilde{S}_2 we obtain the subsystem

$$\begin{aligned} \dot{x} &= x(a_0 + a_1x + a_2z^2 + a_3z), \\ \dot{z} &= c_0z, \end{aligned}$$

which is equivalent to the previous one, taking $\mu = 0$ and interchanging the variables x and z , so it is sufficient to study the Kolmogorov systems (3.2) depending on six parameters.

4. PROPERTIES OF SYSTEM (1.3)

In this section we state some results that will be used on the classification to reduce the number of phase portraits appearing. Note that if $c_2 = 0$, then the system (1.3) is a Lotka-Volterra system in dimension 2. A global topological classification of these systems has been completed in [24], so we limit our study to the case $c_2 \neq 0$.

We recall that for obtaining system (1.3) we have supposed that system (3.1) has the Darboux invariant $I = xz^\mu e^{-t(a_0+c_0\mu)}$, so it is required that $a_0 + c_0\mu \neq 0$.

Proposition 4.1. *Consider system (1.3) and suppose that $(\tilde{x}(t), \tilde{z}(t))$ is a solution of this system. If we change c_1 by $-c_1$ (respectively c_3 by $-c_3$), then $(-\tilde{x}(t), \tilde{z}(t))$ (respectively $(\tilde{x}(t), -\tilde{z}(t))$) is other solution of the obtained system.*

Remark 4.2. By Proposition 4.1 we can limit our study to Kolmogorov systems (1.3) with c_1 and c_3 non-negatives. In the cases with these parameters negatives, we will obtain phase portraits symmetric to the ones obtained in the positive cases, with respect to the z -axis when we change the sign of c_1 , and with respect to the x -axis when we change the sign of c_3 .

Corollary 4.3. *Consider system (1.3) and suppose $(\tilde{x}(t), \tilde{z}(t))$ is a solution. If $c_1 = 0$ (respectively $c_3 = 0$), then $(-\tilde{x}(t), \tilde{z}(t))$ (respectively $(\tilde{x}(t), -\tilde{z}(t))$) is also a solution.*

Remark 4.4. Corollary 4.3 simplifies the study of the cases with $c_1 = 0$ or $c_3 = 0$, because it proves that the phase portraits have to be symmetric with respect to the z -axis and x -axis respectively, and this fact will be useful in obtaining the global phase portraits from the local results.

Proposition 4.5. *Let $(\tilde{x}(t), \tilde{z}(t))$ be a solution of system (1.3). In the next cases we obtain another system with solution $(-\tilde{x}(-t), -\tilde{z}(-t))$.*

- (1) *If a_0, c_0 and c_2 are not zero, and we change the sign of all of them.*
- (2) *If $a_0 = 0$ and we change the sign of c_0 and c_2 , which are not zero.*
- (3) *If $c_0 = 0$ and we change the sign of a_0 and c_2 , which are not zero.*

Remark 4.6. To classify all the phase portraits of the Kolmogorov systems (1.3), according to the previous results, it is sufficient to consider $a_0 \geq 0$. And when $a_0 = 0$ we will consider also $c_0 > 0$.

Remark 4.7. In short, according to the previous results and considerations, from now on it will be sufficient to study the Kolmogorov systems (1.3) with the their parameters satisfying

$$(H2) \quad c_2 \neq 0, a_0 \geq 0, c_1 \geq 0, c_3 \geq 0, a_0 + c_0\mu \neq 0.$$

Theorem 4.8. For system (1.3) the next statements hold.

- (1) If $c_1 \neq 0$, then on any straight line $z = cte \neq 0$, there exists only one contact point.
- (2) If $c_1 = 0$, then there exist two invariant straight lines $z = (\sqrt{c_3^2 - 4c_0c_2} - c_3)/(2c_2)$ and $z = -(\sqrt{c_3^2 - 4c_0c_2} + c_3)/(2c_2)$ if $c_3^2 > 4c_0c_2$, and one invariant straight line $z = -c_3/(2c_2)$ if $c_3^2 = 4c_0c_2$. There are not contact points on any other straight line $z = cte \neq 0$.

Proof. First we suppose $c_1 \neq 0$ and consider a straight line $z = z_0 \neq 0$. Then the contact points on this straight line are those on which $\dot{z} = 0$ and, as $z_0 \neq 0$, the only possible contact point is the one that satisfies $c_0 + c_1x + c_2z_0^2 + c_3z_0 = 0$, i.e. the point such that its first coordinate is $x = -(c_2z_0^2 + c_3z_0 + c_0)/c_1$.

We consider now the case with $c_1 = 0$. Then looking for the points on the straight line $z = z_0 \neq 0$ satisfying $\dot{z} = 0$, we obtain that they must verify the condition $c_0 + c_2z_0^2 + c_3z_0 = 0$, and solving this equation we obtain that either there are no contact points, or a full straight line of contact points, or two straight line of contact points, depending on the solutions z_0 of that equation. \square

5. STUDY OF LOCAL FINITE SINGULAR POINTS

System (1.3) has the following finite singularities:

- $P_0 = (0, 0)$,
- $P_1 = (0, \frac{R_c - c_3}{2c_2})$ and $P_2 = (0, -\frac{R_c + c_3}{2c_2})$ if $c_3^2 > 4c_0c_2$,
- $P_3 = (0, -\frac{c_3}{2c_2})$ if $c_3^2 = 4c_0c_2$,
- $P_4 = (\frac{a_0}{c_1\mu}, 0)$ if $c_1\mu \neq 0$.

We use the notation $R_c = \sqrt{c_3^2 - 4c_0c_2}$ in order to simplify the expressions which will appear. Moreover if $a_0 = 0$ and $c_1\mu = 0$, all the points on the z -axis are singular points, and the system can be reduced to a Lotka-Volterra system in dimension 2. Therefore from now on we will consider the hypothesis

$$(H3) \quad c_2 \neq 0, a_0 \geq 0, c_1 \geq 0, c_3 \geq 0, a_0 + c_0\mu \neq 0, a_0^2 + (c_1\mu)^2 \neq 0.$$

Under this assumption there are 6 different cases according to the finite singular points existing for system (1.3), which are given in Table 1. Then we study the possible local phase portraits in each one of the finite singular points under the hypothesis (H3).

The origin is always an isolated singular point for system (1.3), and we have the next classification for its phase portraits: if $a_0c_0 \neq 0$ the singularity is hyperbolic and two cases are possible, the origin is a saddle point if $c_0 < 0$, and it is an unstable node if $c_0 > 0$. If $a_0 \neq 0$ and $c_0 = 0$ the singularity is semi-hyperbolic and it has two possibilities: if $c_3 \neq 0$ then the origin is a saddle-node, if $c_3 = 0$ and $c_2 < 0$ it

TABLE 1. The different cases for the finite singular points.

Case	Conditions	Finite singular points
1	$c_3^2 > 4c_0c_2, c_1\mu \neq 0.$	$P_0, P_1, P_2, P_4.$
2	$c_3^2 > 4c_0c_2, c_1\mu = 0, a_0 \neq 0.$	$P_0, P_1, P_2.$
3	$c_3^2 = 4c_0c_2, c_1\mu \neq 0.$	$P_0, P_3, P_4.$
4	$c_3^2 = 4c_0c_2, c_1\mu = 0, a_0 \neq 0.$	$P_0, P_3.$
5	$c_3^2 < 4c_0c_2, c_1\mu \neq 0.$	$P_0, P_4.$
6	$c_3^2 < 4c_0c_2, c_1\mu = 0, a_0 \neq 0.$	$P_0.$

is a topological saddle, and if $c_3 = 0$ and $c_2 > 0$ it is a topological unstable node. Finally if $a_0 = 0$ the origin is a semi-hyperbolic saddle-node.

When P_1 is a singular point of system (1.3), it can present different phase portraits. If $c_0 \neq 0$ then P_1 is hyperbolic and it can present the following phase portraits: if $c_2(a_0 + c_0\mu)(R_c - c_3) < 0$ then P_1 is a saddle, if $a_0 + c_0\mu < 0$ and $c_2(R_c - c_3) < 0$ it is a stable node, and finally if $a_0 + c_0\mu > 0$ and $c_2(R_c - c_3) > 0$ it is an unstable node. The singular point P_1 collides with the origin if $c_1 = 0$.

When P_2 is a singular point of system (1.3), it can present three different phase portraits: if $c_2(a_0 + c_0\mu) < 0$ then P_2 is a saddle, if $a_0 + c_0\mu < 0$ and $c_2 < 0$ then it is a stable node, and if $a_0 + c_0\mu > 0$ and $c_2 > 0$ it is an unstable node.

When P_3 is a singularity of system (1.3) it is a semi-hyperbolic saddle-node if $c_3 \neq 0$, and it collides with the origin if $c_3 = 0$.

When P_4 is a singularity of system (1.3) it is hyperbolic if $a_0 \neq 0$ and can present two different phase portraits: if $(a_0 + c_0\mu)\mu > 0$ then P_4 is a saddle, and if $\mu(a_0 + c_0\mu) < 0$ it is a stable node. If $a_0 = 0$ the singularity P_4 collides with the origin.

Lemma 5.1. *Under hypothesis (H3) there are 50 different cases according to the local phase portrait of the finite singular points of system (1.3), which are given in Tables 2–7.*

Proof. We have to analyze cases 1 to 6 in Table 1 and determine the local phase portraits of the singular points existing in each one of them, according to their individual classification. We start with the first one, in which the conditions, $c_3^2 > 4c_0c_2$ and $c_1\mu \neq 0$ hold. The singular points are P_0, P_1, P_2 and P_4 . We shall consider three subcases: $a_0 = 0, c_0 = 0$ and $a_0c_0 \neq 0$.

Consider case $c_0 = 0$ in which the origin is a saddle-node and P_1 collides with the origin. Since $c_0 = 0$ and $a_0 > 0$, the singular point P_2 is a saddle if $c_2 < 0$, and an unstable node if $c_2 > 0$. In these two cases P_4 can be either a saddle if $\mu > 0$, or a stable node if $\mu < 0$. This leads to cases 1.1 to 1.4 in Table 2.

We continue with the case $a_0 = 0$ in which P_0 is again a saddle-node, but in this case it coincides with P_4 . Suppose that P_1 is an unstable node, then we have $c_0\mu > 0$ and $c_2(R_c - c_3) > 0$. By Remark 4.6 we will only consider the case $c_0 > 0$. Then if $c_2 > 0$ and $R_c - c_3 > 0$ taking into account the expression of R_c and squaring both terms, we obtain that $c_3^2 - 4c_0c_2 > c_3^2$, so $c_0c_2 < 0$, which leads to a contradiction. The same occurs if we suppose $c_2 < 0$. Therefore P_1 cannot be an unstable node. If P_1 is a saddle, then P_2 can be a saddle or an unstable node, but not a stable node, which is only possible if $c_0 < 0$, by an analogous reasoning

to the previous one. If P_1 is a stable node then $c_0\mu < 0$, so P_2 can be a saddle or stable node, but not an unstable node because it requires that $c_0\mu > 0$. This leads to cases 1.5 to 1.8.

The last case is $a_0c_0 \neq 0$ in which the origin is a hyperbolic singular point. We start when P_0 is a saddle, then $c_0 < 0$. First we consider that P_1 is also a saddle, and so $c_2(a_0 + c_0\mu)(R_c - c_3) < 0$. If P_2 is a saddle then $c_2(a_0 + c_0\mu) < 0$, and we obtain $R_c - c_3 > 0$. From this we deduce like in previous cases that $c_0c_2 < 0$, but we are supposing $c_0 < 0$ and so $c_2 > 0$ and $a_0 + c_0\mu < 0$. From the last inequality $a_0 < -c_0\mu$, and so μ has to be positive. In short $\mu(a_0 + c_0\mu) < 0$, and consequently P_4 can only be a stable node. If P_0 and P_1 are saddles, but P_2 is a stable node, reasoning in an analogous way we obtain that P_4 is again a stable node. This leads to cases 1.9 and 1.10. Note that if P_0 and P_1 are saddles it is impossible for P_2 to be an unstable node. In that case we would have that $c_0 < 0$, $c_2 > 0$, $a_0 + c_0\mu > 0$ and $R_c - c_3 < 0$. From this last inequality we obtain that $c_0c_2 > 0$, which is a contradiction. We consider now the cases where P_0 is a saddle and P_1 an unstable node, in which the conditions $c_0 < 0$, $a_0 + c_0\mu > 0$ and $c_2(R_c - c_3) > 0$ hold. It is obvious that P_2 cannot be a stable node because it requires that $a_0 + c_0\mu < 0$, so P_2 is a saddle if $c_2 < 0$ and an unstable node if $c_2 > 0$. In both cases P_4 can be either a saddle if $\mu > 0$, or a stable node if $\mu < 0$. This leads to cases 1.11 to 1.14. Note that the case with P_0 a saddle and P_1 a stable node is not possible, because we would have $c_0 < 0$, $a_0 + c_0\mu < 0$ and $c_2(R_c - c_3) < 0$. If $c_2 > 0$ then $R_c - c_3 < 0$, whence we deduce $c_0c_2 > 0$ and get a contradiction. The same argument is valid if $c_2 < 0$. With analogous reasoning as in the case where P_0 is an unstable node we obtain the subcases 1.15 to 1.20.

Now we study case 2 of Table 1, in which $c_3^2 > 4c_0c_2$, $c_1\mu = 0$, and $a_0 \neq 0$. We shall consider three cases: $c_0 < 0$, $c_0 > 0$, and $c_0 = 0$.

We start with case $c_0 < 0$ in which P_0 is a saddle. If P_1 is a saddle, then P_2 can be a saddle or a stable node. If P_2 is an unstable node, then we have the conditions $c_2(a_0 + c_0\mu)(R_c - c_3) < 0$, $c_2 > 0$, and $a_0 + c_0\mu > 0$, so $R_c - c_3 < 0$, and we deduce $c_0c_2 > 0$ which is a contradiction. P_1 cannot be a stable node, because in that case we would have the conditions $c_0 < 0$, $a_0 + c_0\mu < 0$, and $c_2(R_c - c_3) < 0$ which lead to a contradiction in the following way: if $c_2 > 0$ then $R_c - c_3 < 0$ and squaring we deduce $c_0c_2 > 0$ which is not possible because $c_0 < 0$ and we are supposing $c_2 > 0$. An analogous reasoning works in the case $c_2 < 0$. If P_1 is an unstable node then P_2 can be either a saddle or an unstable node, but not a stable node because it requires $a_0 + c_0\mu$ to be negative, but we already know that this expression is positive because it is a condition in order that P_1 be an unstable node. This leads to cases 2.1 to 2.4 of Table 3.

We continue with the case $c_0 > 0$, in which P_0 is an unstable node. If P_1 is a saddle, then P_2 can be a saddle or an unstable node. If P_2 is a stable node then we have the conditions $c_0 > 0$, $c_2(a_0 + c_0\mu)(R_c - c_3) < 0$, $a_0 + c_0\mu < 0$ and $c_2 < 0$. Thus we have $R_c - c_3 < 0$ and squaring we obtain $c_0c_2 > 0$ which is a contradiction. This leads to cases 2.5 and 2.6. If P_1 is a stable node it can be proved similarly to previous cases, that P_2 cannot be an unstable node. This leads to cases 2.7 and 2.8. P_1 cannot be an unstable node, because in that case we would have the conditions $c_0 > 0$, $a_0 + c_0\mu > 0$ and $c_2(R_c - c_3) > 0$ which lead to a contradiction in the following way: if $c_2 > 0$ then $R_c - c_3 > 0$, and squaring we deduce $c_0c_2 < 0$

which is not possible because $c_0 > 0$ and we are supposing $c_2 > 0$. An analogous reasoning works in the case $c_2 < 0$.

At last we have the case $c_0 = 0$. Necessarily $c_3 \neq 0$ so the origin is a saddle-node. Also we have that P_1 coincides with the origin. For the singular point P_2 we have that it is a saddle if $c_2 < 0$, and an unstable node if $c_2 > 0$. This leads to cases 2.9 and 2.10.

We study case 3 of Table 1 in which $c_3^2 = 4c_0c_2$ and $c_1\mu \neq 0$. Then $c_0 = 0$ if and only if $c_3 = 0$. We consider $a_0 > 0$ and $c_0 < 0$, then the origin is a saddle and P_3 a saddle-node (as $c_3 \neq 0$). The singular point P_4 is either a saddle or a stable node, depending on the sign of $\mu(a_0 + c_0\mu)$. The same is valid in the case $a_0 > 0$ and $c_0 < 0$, except for the origin which is now an unstable node. We get the cases 3.1 to 3.4 of Table 4. We continue with the case in which $a_0 = 0$ and so P_0 is a saddle-node, P_4 coincides with P_0 and P_3 is a saddle-node. This correspond with case 3.5. At last we have the condition $c_0 = 0$, under which P_3 coincides with P_0 . If $c_2 < 0$ then it is a topological saddle, and if $c_2 > 0$ it is a topological unstable node. In any case P_4 can be either a saddle or a stable node. This leads to cases 3.6 to 3.9.

Now we address the case 4 of Table 1 in which $c_3^2 = 4c_0c_2$, $c_1\mu = 0$, and $a_0 \neq 0$. The origin is a saddle if $c_0 < 0$, and an unstable node if $c_0 > 0$. If $c_0 = 0$ then $c_3 = 0$, so we distinguish two semi-hyperbolic possibilities for the origin: if $c_2 < 0$ it is a topological saddle, and if $c_2 > 0$ it is a topological unstable node. The classification of P_3 is totally determined by the one of P_0 , because it only depends on whether c_3 is zero or not. We get cases 4.1 to 4.4.

In case 5 of Table 1 the conditions $c_3^2 < 4c_0c_2$ and $c_1\mu \neq 0$ hold. The singular points are P_0 and P_4 . From condition $c_3^2 < 4c_0c_2$ we obtain that $c_0 \neq 0$. If $a_0 = 0$ then the origin is a saddle-node and P_4 coincides with the origin. If $a_0 \neq 0$ then both singular points are hyperbolic, and it leads to cases 5.2 to 5.5.

Finally in case 6 of Table 1 we have the conditions $c_3^2 < 4c_0c_2$, $c_1\mu = 0$, and $a_0 \neq 0$. The unique singular point is the origin and as c_0 cannot be zero, it is either a saddle or an unstable node. \square

6. STUDY OF LOCAL INFINITE SINGULAR POINTS

To study the behavior of the trajectories of system (1.3) near infinity we consider its Poincaré compactification. For the moment we assume the same hypothesis (H3) than in previous sections. According to equations (2.1) and (2.2), we obtain the compactification in the local charts U_1 and U_2 respectively. From Section 2 it is enough to study the singular points over $v = 0$ in the chart U_1 and the origin of the chart U_2 .

In chart U_1 system (1.3) writes

$$\begin{aligned}\dot{u} &= c_2(\mu + 1)u^3 + c_3(\mu + 1)u^2v + (c_0 - a_0)uv^2 + c_1(\mu + 1)uv, \\ \dot{v} &= c_2\mu u^2v + c_3\mu uv^2 - a_0v^3 + c_1\mu v^2.\end{aligned}\tag{6.1}$$

Taking $v = 0$ we obtain $\dot{u}|_{v=0} = c_2(\mu + 1)u^3$ and $\dot{v}|_{v=0} = 0$. Therefore if $\mu = -1$ all points at infinity are singular points, and we will not deal with this situation in this paper. In other case, if $\mu \neq -1$ the only singular point is the origin of U_1 , which we denote by O_1 . The linear part of system (6.1) at the origin is identically zero, so we must use the blow-up technique to study it, leading to the following result

TABLE 2. Classification in case 1 of Table 1 according to the local phase portraits of finite singular points.

Case 1: $c_3^2 > 4c_0c_2$, $c_1\mu \neq 0$.

Sub.	Conditions	Classification
1.1	$a_0 > 0, c_0 = 0, \mu > 0, c_2 < 0$.	$P_0 \equiv P_1$ saddle-node, P_2 saddle, P_4 saddle.
1.2	$a_0 > 0, c_0 = 0, \mu > 0, c_2 > 0$.	$P_0 \equiv P_1$ saddle-node, P_2 unstable node, P_4 saddle.
1.3	$a_0 > 0, c_0 = 0, \mu < 0, c_2 < 0$.	$P_0 \equiv P_1$ saddle-node, P_2 saddle, P_4 stable node.
1.4	$a_0 > 0, c_0 = 0, \mu < 0, c_2 > 0$.	$P_0 \equiv P_1$ saddle-node, P_2 unstable node, P_4 stable node.
1.5	$a_0 = 0, c_0 > 0, c_2\mu < 0, R_c - c_3 > 0$.	$P_0 \equiv P_4$ saddle-node, P_1 saddle, P_2 saddle.
1.6	$a_0 = 0, c_0 > 0, R_c - c_3 < 0, \mu > 0, c_2 > 0$.	$P_0 \equiv P_4$ saddle-node, P_1 saddle, P_2 unstable node.
1.7	$a_0 = 0, c_0 > 0, \mu < 0, R_c - c_3 < 0, c_2 > 0$.	$P_0 \equiv P_4$ saddle-node, P_1 stable node, P_2 saddle.
1.8	$a_0 = 0, c_0 > 0, \mu < 0, c_2 < 0, R_c - c_3 > 0$.	$P_0 \equiv P_4$ saddle-node, P_1 stable node, P_2 stable node.
1.9	$a_0 > 0, c_0 < 0, \mu > 0, (a_0 + c_0\mu) < 0, c_2 > 0, R_c - c_3 > 0$.	P_0 saddle, P_1 saddle, P_2 saddle, P_4 stable node.
1.10	$a_0 > 0, c_0 < 0, c_2 < 0, \mu > 0, a_0 + c_0\mu < 0, R_c - c_3 < 0$.	P_0 saddle, P_1 saddle, P_2 stable node, P_4 stable node.
1.11	$a_0 > 0, c_0 < 0, c_2 < 0, \mu > 0, a_0 + c_0\mu > 0, (R_c - c_3) < 0$.	P_0 saddle, P_1 unstable node, P_2 saddle, P_4 saddle.
1.12	$a_0 > 0, c_0 < 0, c_2 < 0, \mu < 0, a_0 + c_0\mu > 0, (R_c - c_3) < 0$.	P_0 saddle, P_1 unstable node, P_2 saddle, P_4 stable node.
1.13	$a_0 > 0, c_0 < 0, \mu > 0, a_0 + c_0\mu > 0, c_2 > 0, R_c - c_3 > 0$.	P_0 saddle, P_1 unstable node, P_2 unstable node, P_4 saddle.
1.14	$a_0 > 0, c_0 < 0, \mu < 0, a_0 + c_0\mu > 0, c_2 > 0, R_c - c_3 > 0$.	P_0 saddle, P_1 unstable node, P_2 unstable node, P_4 stable node.
1.15	$a_0 > 0, c_0 > 0, \mu(a_0 + c_0\mu) > 0, c_2(a_0 + c_0\mu) < 0, R_c - c_3 > 0$.	P_0 unstable node, P_1 saddle, P_2 saddle, P_4 saddle.
1.16	$a_0 > 0, c_0 > 0, \mu(a_0 + c_0\mu) < 0, c_2(a_0 + c_0\mu) < 0, R_c - c_3 > 0$.	P_0 unstable node, P_1 saddle, P_2 saddle, P_4 stable node.
1.17	$a_0 > 0, c_0 > 0, \mu > 0, R_c - c_3 < 0, a_0 + c_0\mu > 0, c_2 > 0$.	P_0 unstable node, P_1 saddle, P_2 unstable node, P_4 saddle.
1.18	$a_0 > 0, c_0 > 0, \mu < 0, R_c - c_3 < 0, a_0 + c_0\mu > 0, c_2 > 0$.	P_0 unstable node, P_1 saddle, P_2 unstable node, P_4 stable node.
1.19	$a_0 > 0, c_0 > 0, \mu < 0, a_0 + c_0\mu < 0, R_c - c_3 < 0, c_2 > 0$.	P_0 unstable node, P_1 stable node, P_2 saddle, P_4 saddle.
1.20	$a_0 > 0, c_0 > 0, \mu < 0, a_0 + c_0\mu < 0, c_2 < 0, R_c - c_3 > 0$.	P_0 unstable node, P_1 stable node, P_2 stable node, P_4 saddle.

which is proved in Subsections 6.1 and 6.2. From now on we include the condition

TABLE 3. Classification in case 2 of Table 1 according to the local phase portraits of finite singular points.

Case 2: $c_3^2 > 4c_0c_2$, $c_1\mu = 0$, $a_0 > 0$.

Sub.	Conditions	Classification
2.1	$c_0 < 0$, $c_2(a_0 + c_0\mu) < 0$, $R_c - c_3 > 0$.	P_0 saddle, P_1 saddle, P_2 saddle.
2.2	$c_0 < 0$, $R_c - c_3 < 0$, $a_0 + c_0\mu < 0$, $c_2 < 0$.	P_0 saddle, P_1 saddle, P_2 stable node.
2.3	$c_0 < 0$, $a_0 + c_0\mu > 0$, $R_c - c_3 < 0$, $c_2 < 0$.	P_0 saddle, P_1 unstable node, P_2 saddle.
2.4	$c_0 < 0$, $a_0 + c_0\mu > 0$, $c_2 > 0$, $R_c - c_3 > 0$.	P_0 saddle, P_1 unstable node, P_2 unstable node.
2.5	$c_0 > 0$, $c_2(a_0 + c_0\mu) < 0$, $R_c - c_3 > 0$.	P_0 unstable node, P_1 saddle, P_2 saddle.
2.6	$c_0 > 0$, $R_c - c_3 < 0$, $a_0 + c_0\mu > 0$, $c_2 > 0$.	P_0 unstable node, P_1 saddle, P_2 unstable node.
2.7	$c_0 > 0$, $a_0 + c_0\mu < 0$, $R_c - c_3 < 0$, $c_2 > 0$.	P_0 unstable node, P_1 stable node, P_2 saddle.
2.8	$c_0 > 0$, $a_0 + c_0\mu < 0$, $c_2 < 0$, $R_c - c_3 > 0$.	P_0 unstable node, P_1 stable node, P_2 stable node.
2.9	$c_0 = 0$, $a_0 > 0$, $c_2 < 0$.	$P_0 \equiv P_1$ saddle-node, P_2 saddle.
2.10	$c_0 = 0$, $a_0 > 0$, $c_2 > 0$.	$P_0 \equiv P_1$ saddle-node, P_2 unstable node.

$\mu \neq -1$ in our hypothesis, so we will work under the condition (H1):

$$c_2 \neq 0, \quad a_0 \geq 0, \quad c_1 \geq 0, \quad c_3 \geq 0, \quad a_0 + c_0\mu \neq 0, \quad a_0c_1\mu \neq 0, \quad \mu \neq -1.$$

Lemma 6.1. *Under assumption (H1) the origin of the chart U_1 is an infinite singular point of system (1.3), and it has 47 distinct local phase portraits described in Figure 1.*

For system (6.1), if $c_1 \neq 0$ the characteristic polynomial is $\mathcal{F} = -c_1uv^2 \neq 0$, so the origin is a nondicritical singular point. If $c_1 = 0$ the characteristic polynomial is $\mathcal{F} = -c_3u^2v - c_2u^3v - c_0uw^3$, which cannot be identically zero because $c_2 \neq 0$. We will study this two cases separately.

6.1. Case c_1 non-zero. Consider $c_1 \neq 0$. We introduce the new variable w_1 by means of the variable change $uw_1 = v$, and get the system

$$\begin{aligned} \dot{u} &= (c_0 - a_0)u^3w_1^2 + c_3(\mu + 1)u^3w_1 + c_2(\mu + 1)u^3 + c_1(\mu + 1)u^2w_1, \\ \dot{w}_1 &= -c_0u^2w_1^3 - c_3u^2w_1^2 - c_2u^2w_1 - c_1uw_1^2. \end{aligned} \quad (6.2)$$

Now we cancel the common factor u , getting the system

$$\begin{aligned} \dot{u} &= (c_0 - a_0)u^2w_1^2 + c_3(\mu + 1)u^2w_1 + c_2(\mu + 1)u^2 + c_1(\mu + 1)uw_1, \\ \dot{w}_1 &= -c_0uw_1^3 - c_3uw_1^2 - c_2uw_1 - c_1w_1^2, \end{aligned} \quad (6.3)$$

for which the only singular point on the exceptional divisor is the origin, and it is linearly zero, so we have to repeat the process. Now the characteristic polynomial is $\mathcal{F} = -c_2(\mu + 2)u^2w_1 - c_1(\mu + 2)uw_1^2$, so the origin is a nondicritical singular

TABLE 4. Classification in case 3 of Table 1 according to the local phase portraits of finite singular points.

Case 3: $c_3^2 = 4c_0c_2$, $c_1\mu \neq 0$.

Sub.	Conditions	Classification
3.1	$a_0 > 0$, $c_0 < 0$, $\mu(a_0 + c_0\mu) > 0$.	P_0 saddle, P_3 saddle-node, P_4 saddle.
3.2	$a_0 > 0$, $c_0 < 0$, $\mu(a_0 + c_0\mu) < 0$.	P_0 saddle, P_3 saddle-node, P_4 stable node.
3.3	$a_0 > 0$, $c_0 > 0$, $\mu(a_0 + c_0\mu) > 0$.	P_0 unstable node, P_3 saddle-node, P_4 saddle.
3.4	$a_0 > 0$, $c_0 > 0$, $\mu(a_0 + c_0\mu) < 0$.	P_0 unstable node, P_3 saddle-node, P_4 stable node.
3.5	$a_0 = 0$, $c_0 > 0$.	$P_0 \equiv P_4$ saddle-node, P_3 saddle-node.
3.6	$c_0 = 0$, $a_0 > 0$, $c_2 < 0$, $\mu > 0$.	$P_0 \equiv P_3$ topological saddle, P_4 saddle.
3.7	$c_0 = 0$, $a_0 > 0$, $c_2 < 0$, $\mu < 0$.	$P_0 \equiv P_3$ topological saddle, P_4 stable node.
3.8	$c_0 = 0$, $a_0 > 0$, $c_2 > 0$, $\mu > 0$.	$P_0 \equiv P_3$ topological unstable node, P_4 saddle.
3.9	$c_0 = 0$, $a_0 > 0$, $c_2 > 0$, $\mu < 0$.	$P_0 \equiv P_3$ topological unstable node, P_4 stable node.

TABLE 5. Classification in case 4 of Table 1 according to the local phase portraits of finite singular points.

Case 4: $c_3^2 = 4c_0c_2$, $c_1\mu = 0$, $a_0 > 0$.

Sub.	Conditions	Classification
4.1	$c_0 < 0$.	P_0 saddle, P_3 saddle-node.
4.2	$c_0 > 0$.	P_0 unstable node, P_3 saddle-node.
4.3	$c_0 = 0$, $c_2 < 0$.	$P_0 \equiv P_3$ topological saddle.
4.4	$c_0 = 0$, $c_2 > 0$.	$P_0 \equiv P_3$ topological unstable node.

TABLE 6. Classification in case 5 of Table 1 according to the local phase portraits of finite singular points.

Case 5: $c_3^2 < 4c_0c_2$, $c_1\mu \neq 0$.

Sub.	Conditions	Classification
5.1	$a_0 = 0$.	$P_0 \equiv P_4$ saddle-node.
5.2	$a_0 > 0$, $c_0 < 0$, $\mu(a_0 + c_0\mu) > 0$.	P_0 saddle, P_4 saddle.
5.3	$a_0 > 0$, $c_0 < 0$, $\mu(a_0 + c_0\mu) < 0$.	P_0 saddle, P_4 stable node.
5.4	$a_0 > 0$, $c_0 > 0$, $\mu(a_0 + c_0\mu) > 0$.	P_0 unstable node, P_4 saddle.
5.5	$a_0 > 0$, $c_0 > 0$, $\mu(a_0 + c_0\mu) < 0$.	P_0 unstable node, P_4 stable node.

point if $\mu \neq -2$, and it is dicritical if $\mu = -2$. In both cases we introduce the new

TABLE 7. Classification in case 6 of Table 1 according to the local phase portraits of finite singular points.

Case 6: $c_3^2 < 4c_0c_2$, $c_1\mu = 0$, $a_0 > 0$.

Sub.	Conditions	Classification
6.1	$c_0 < 0$.	P_0 saddle.
6.2	$c_0 > 0$.	P_0 unstable node.

variable w_2 doing the change $uw_2 = w_1$, obtaining the system

$$\begin{aligned} \dot{u} &= (c_0 - a_0)u^4w_2^2 + c_3(\mu + 1)u^3w_2 + c_2(\mu + 1)u^2 + c_1(\mu + 1)u^2w_2, \\ \dot{w}_2 &= (a_0 - 2c_0)u^3w_2^3 - c_3(\mu + 2)u^2w_2^2 - c_1(\mu + 2)uw_2^2 - c_2(\mu + 2)uw_2. \end{aligned} \quad (6.4)$$

In the nondicritical case we have to cancel the common factor u obtaining

$$\begin{aligned} \dot{u} &= (c_0 - a_0)u^3w_2^2 + c_3(\mu + 1)u^2w_2 + c_2(\mu + 1)u + c_1(\mu + 1)uw_2, \\ \dot{w}_2 &= (a_0 - 2c_0)u^2w_2^3 - c_3(\mu + 2)uw_2^2 - c_1(\mu + 2)w_2^2 - c_2(\mu + 2)w_2. \end{aligned} \quad (6.5)$$

But in the dicritical case, when $\mu = -2$, we must cancel the common factor u^2 from system (6.4), and we obtain the system

$$\begin{aligned} \dot{u} &= (c_0 - a_0)u^2w_2^2 - c_3uw_2 - c_2 - c_1w_2, \\ \dot{w}_2 &= (a_0 - 2c_0)uw_2^3. \end{aligned} \quad (6.6)$$

6.1.1. *Nondicritical case.* In this case it is necessary to study the singular points of system (6.5) on the exceptional divisor. The origin is always a singular point, and we denote it by Q_0 . As $\mu + 2 \neq 0$ there is another singular point, $Q_1 = (0, -c_2/c_1)$ and we determine their local phase portraits.

The origin Q_0 is always hyperbolic. It is a saddle if $\mu \in (-\infty, -2) \cup (-1, +\infty)$, a stable node if $c_2 > 0$ and $\mu \in (-2, -1)$, and an unstable node if $c_2 < 0$ and $\mu \in (-2, -1)$.

The singular point Q_1 is semi-hyperbolic. If $c_2(a_0 + c_0\mu) > 0$ then Q_1 is a topological saddle, if $c_2(\mu + 2) > 0$ and $(\mu + 2)(a_0 + c_0\mu) < 0$ then it is a topological unstable node, and if $c_2(\mu + 2) < 0$ and $(\mu + 2)(a_0 + c_0\mu) > 0$ it is a topological stable node. These conditions come together in the next 7 subcases.

(1) If $\mu \in (-\infty, -2) \cup (-1, +\infty)$ and $c_2(a_0 + c_0\mu) > 0$, then Q_0 is a saddle and Q_1 a topological saddle. To determine the phase portrait around the w_2 -axis for system (6.5), we must fix the sign of c_2 , which determines the position of the singular point Q_1 , and also the sign of $\mu + 1$, which determines the sense of the flow along the x -axis. Thus we deal with the following subcases.

Subcase (1.1). Let $\mu < -2$ (so $\mu + 1 < 0$) and $c_2 > 0$. Then the singular point Q_1 is on the negative part of the w_2 -axis and the expression $\dot{u}|_{w_2=0} = c_2(\mu + 1)u$ determines the sense of the flow, so the phase portrait is the one in Figure 2(a).

To return to system (6.4) we multiply by u , thus the orbits in the second and third quadrants change their orientation. Moreover all the points on the w_2 -axis become singular points. The resultant phase portrait is given in Figure 2(b).

When going back to the (u, w_1) -plane the second and the third quadrants swap from the (u, w_2) -plane, and the exceptional divisor shrinks to a point, and hence the orbits are slightly modified. Attending to the expressions of $\dot{u}|_{w_1=0} = c_2(\mu + 1)u^2$ and $\dot{w}_1|_{u=0} = -c_1w_1^2$, we know the sense of the flow along the axes. Following the results

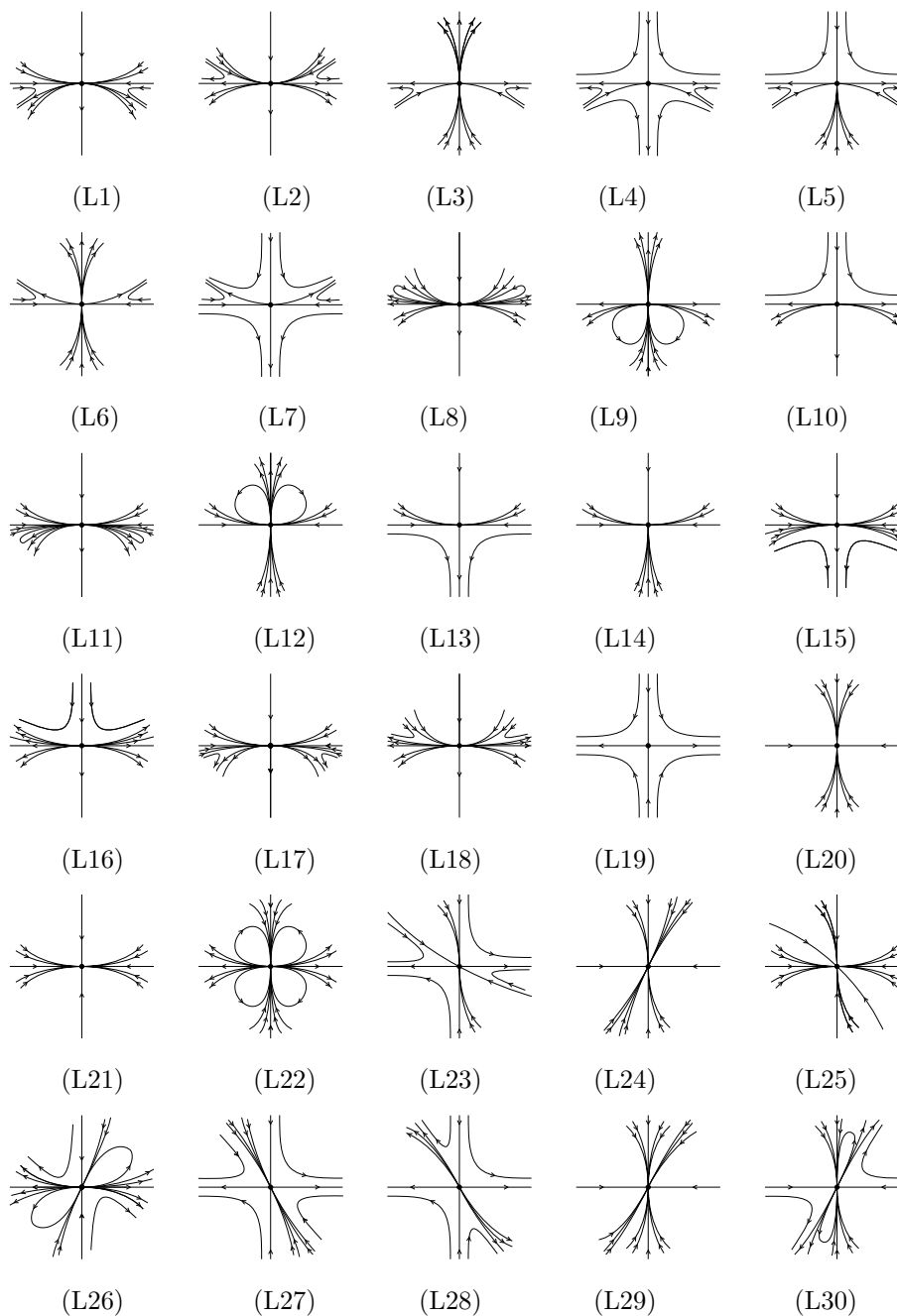


FIGURE 1. Local phase portraits of the infinite singular point O_1
(to be continued)

mentioned in Subsection 2.3, the separatrix of the singular point $Q_1 = (0, -c_2/c_1)$ in the (u, w_2) -plane, becomes the separatrix with slope $-c_2/c_1$ in the (u, w_1) -plane.

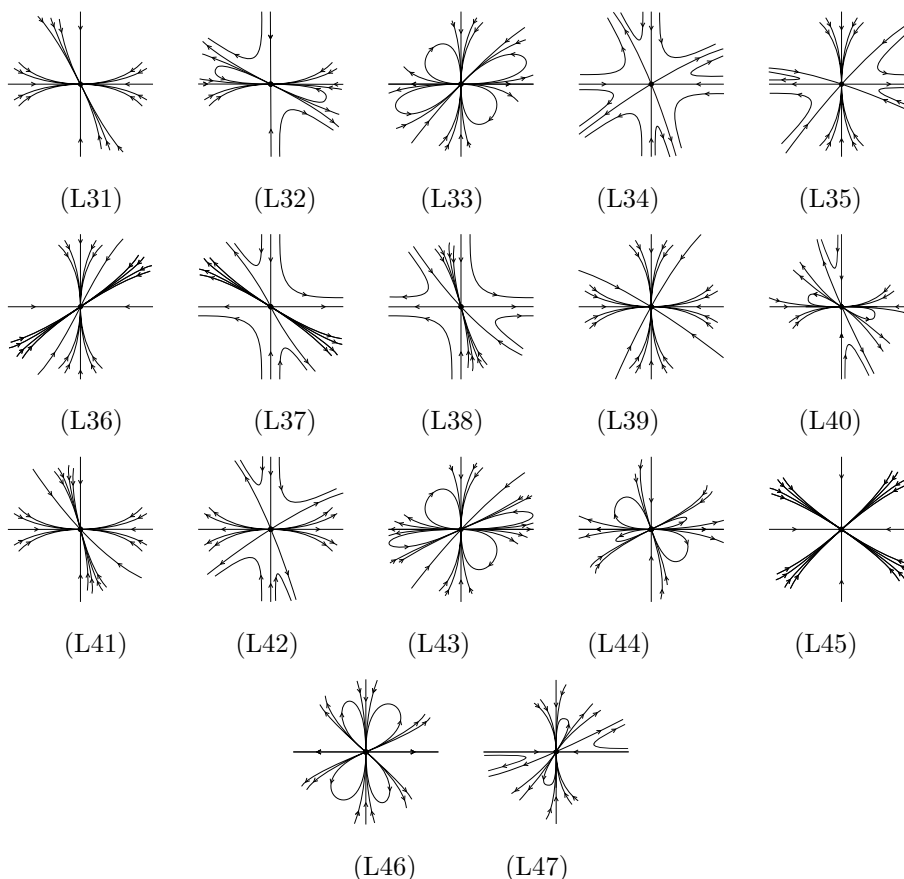


FIGURE 1. (cont.) Local phase portraits of the infinite singular point O_1 .

We get the phase portrait given in Figure 2(c), and multiplying again by u , the one given in Figure 2(d).

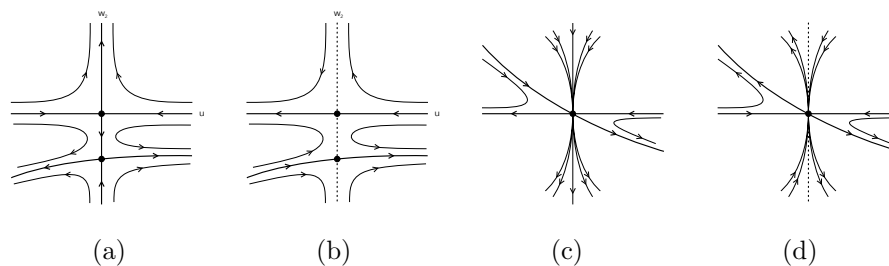


FIGURE 2. Desingularization of the origin of system (6.1) with $c_1 \neq 0$. Nondcritical case (1.1).

Finally we must go back to the (u, v) -plane, swapping the second and the third quadrants and contracting the exceptional divisor to the origin. The orbits tending

to the origin in forward or backward time, became orbits tending to the origin in forward or backward time with slope zero, i.e. tangent to the u -axis. According to the expressions $\dot{u}|_{v=0} = c_1\mu v^2 - a_0v^3$ and $\dot{u}|_{v=0} = c_2(\mu + 1)u^3$, which determine the sense of the flow along the axes, we obtain the local phase portrait at the origin for system (6.1) given in Figure 1(L1).

Subcase (1.2) If we maintain $\mu < -2$ but take $c_2 < 0$, the reasoning is essentially similar to the one we have given in the previous case, and we obtain the phase portrait (L2) of Figure 1.

Subcase (1.3) Let $\mu > -1$ and $c_2 > 0$. This determines the position of the singular point Q_1 and the sense of the flow along the axes, so around the w_2 -axis we obtain the phase portrait given in Figure 3(a).

As in the previous subcase we multiply by u obtaining the phase portrait given in Figure 3(b), as the orbits in the second and third quadrants change their orientation and all the point in the w_2 -axis become singular points.

To undo the variable change we analyze the sense of the flow along the axes according to the expression $\dot{u}|_{w_1=0} = c_2(\mu + 1)u^2$, which determines that the flow goes in the positive sense of the u -axis, and $\dot{w}_1|_{u=0} = -c_1w_1^2$ which determines that the flow goes in the negative sense of the w_1 -axis. Moreover we swap the second and third quadrants, and press the exceptional divisor into the origin, modifying the orbits. We obtain the phase portrait given in Figure 3(c). Multiplying again by u we obtain the phase portrait 3(d).

Now we have to undo de second variable change. We note that $\dot{u}|_{v=0} = c_2(\mu + 1)u^3$, so the flow gets away from the origin along the u -axis, nevertheless the sense of the flow along the v -axis is not determined by $\dot{v}|_{u=0} = c_1\mu v^2 - a_0v^3$, it depends on the constant μ . If $\mu > 0$ the flow goes in the positive sense of the v -axis, if $\mu < 0$ in the opposite sense and, if $\mu = 0$ the flow goes to the origin. Thus we must distinguish three subcases and in each of them, modifying the orbits properly, we obtain, respectively, the phase portraits given in Figure 1(L3), (L4) and (L5).

Subcase (1.4). Let $\mu > -1$ and $c_2 < 0$. By a similar reasoning to the previous one, we obtain the phase portraits (L6) and (L7) of Figure 1.

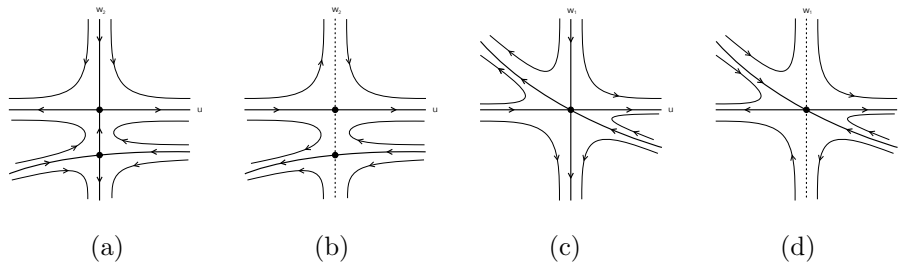


FIGURE 3. Desingularization of the origin of system (6.1) with $c_1 \neq 0$. Nondicritical case (1.3).

(2) If $\mu \in (-\infty, -2) \cup (-1, +\infty)$, $c_2(\mu + 2) > 0$ and $(\mu + 2)(a_0 + c_0\mu) < 0$, then Q_0 is a saddle and Q_1 a topological unstable node. We must distinguish two cases according to the sign of c_2 .

Subcase (2.1). We consider $c_2 < 0$ so $\mu < -2$ and $a_0 + c_0\mu > 0$. The singular point Q_1 is on the positive w_2 -axis and it is an unstable node, so the sense of the

flow along the axes is determined, and we obtain the phase portrait given in Figure 4(a). Multiplying by u we obtain Figure 4(b).

We see that for system (6.3) the flow goes in the negative sense along the w_1 -axis and in the positive sense along the u -axis, according to the expressions $\dot{u}|_{w_1=0} = c_2(\mu + 1)u^2$ and $\dot{w}_1|_{u=0} = -c_1w_1^2$. We undo the variable change modifying the orbits properly, and we note that it must exist an hyperbolic or elliptic sector in both first and third quadrants, thus it can appear the configuration given in Figure 4(c) or the one given in Figure 5(a). From the first of them multiplying by u we obtain 4(d), and if we undo the variable change in a similarly way than in the previous cases, we obtain the phase portrait in Figure 1(L8).

If we consider hyperbolic sectors we continue undoing the blow up from Figure 5(a), obtaining successively the phase portraits 5(b) and 5(c). However in our study we have proved, by means of the index theory, that only the case with elliptic sectors is feasible in the global phase portraits obtained. More detailed explanations will be given in Section 7 but, roughly speaking we know that the index of the vector field on the sphere must be 2, and this index is the sum of the indices of all singularities, which depend on the sectors that they have, so if the index is 2 considering two elliptic sectors in a particular singular point, it cannot be 2 if we change those sectors for hyperbolic ones. In conclusion the only phase portrait that will appear in this case is (L8) of Figure 1.

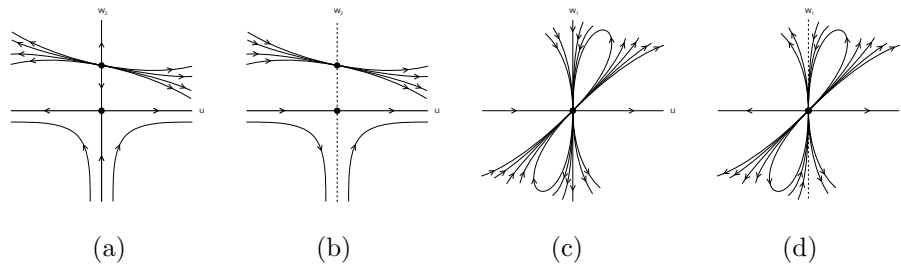


FIGURE 4. Desingularization of the origin of system (6.1) with $c_1 \neq 0$. Nondicritical case (2.1).

From now on we will omit the reasonings about how to undo the variable changes for obtaining the final phase portrait, because they are similar to the ones of the previous cases. The results obtained are the following.

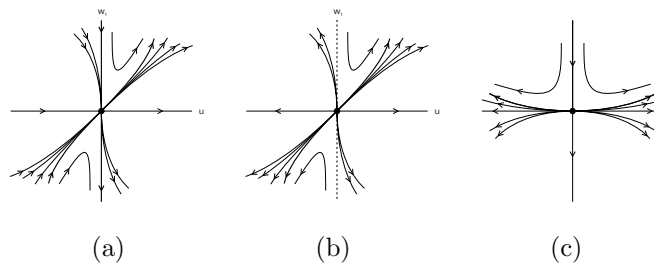


FIGURE 5. Desingularization of the origin of system (6.1) with $c_1 \neq 0$. Alternative to nondicritical case (2.1).

Subcase (2.2). Let $c_2 > 0$ so $\mu > -1$ and $a_0 + c_0\mu < 0$. We obtain the phase portraits (L9) and (L10) of Figure 1. In (L9) it is possible to consider hyperbolic sectors instead of the elliptic ones, but applying index theory to the global phase portraits obtained in our study, we note that only the phase portrait with elliptic sectors is feasible.

(3) If $\mu \in (-\infty, -2) \cup (-1, +\infty)$, $c_2(\mu + 2) < 0$ and $(\mu + 2)(a_0 + c_0\mu) > 0$, then Q_0 is a saddle and Q_1 a topological stable node. If $c_2 > 0$ we obtain the phase portrait (L11) of Figure 1, and if $c_2 < 0$ we obtain the phase portraits (L12), (L13) and (L14) of Figure 1. In (L11) and (L12) it would be possible that the elliptic sectors appearing were hyperbolic sectors, but again we have proved that only the elliptic option is feasible according to the index theory.

(4) If $c_2 > 0$, $\mu \in (-2, -1)$ and $a_0 + c_0\mu > 0$, then Q_0 is a stable node and Q_1 a topological saddle. We obtain the phase portrait (L15) of Figure 1.

(5) If $c_2 > 0$, $\mu \in (-2, -1)$ and $a_0 + c_0\mu < 0$, then Q_0 is a stable node and Q_1 a topological unstable node. We obtain the phase portrait (L11) of Figure 1.

(6) If $c_2 < 0$, $\mu \in (-2, -1)$ and $a_0 + c_0\mu < 0$, then Q_0 is an unstable node and Q_1 a topological saddle. We obtain the phase portrait (L16) of Figure 1.

(7) If $c_2 < 0$, $\mu \in (-2, -1)$ and $a_0 + c_0\mu > 0$, then Q_0 is an unstable node and Q_1 a topological stable node. We obtain the phase portrait (L8) of Figure 1.

6.1.2. *Dicritical case.* Now we must study the singular points on the exceptional divisor of system (6.6). In this case there is only one singular point, $R = (0, -c_2/c_1)$ which is non-degenerated. We shall distinguish several subcases.

- If $c_3^2 < -4c_2(a_0 - 2c_0)$ and $c_2c_3 < 0$, then P is a stable focus. We shall distinguish two cases depending on the sign of the parameter c_2 , because it determines if the singular point is on the positive or negative u -axis. We consider $c_2 > 0$. In Figure 6 the blowing-down process is represented. The phase portrait around the u -axis is the one given in Figure 6(a), multiplying by u^2 we obtain (b), undoing the second variable change we obtain (c), multiplying by u we obtain (d) and finally, undoing the first variable change we obtain the phase portrait (L11) of Figure 1. Taking $c_2 < 0$ and by the same method we obtain the phase portrait (L8) of Figure 1.

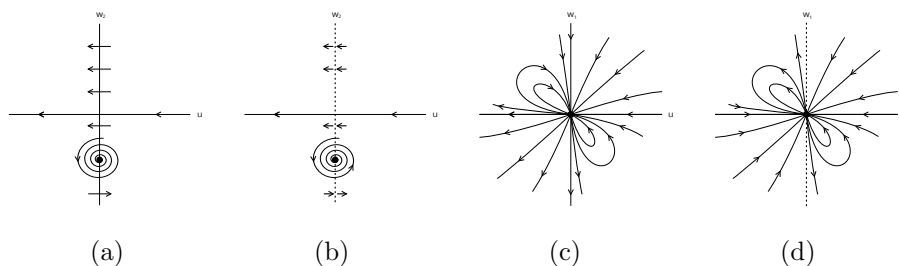


FIGURE 6. Desingularization of the origin of system (6.1) with $c_1 \neq 0$. Dicritical case (1), $c_2 > 0$.

From now on we omit explanations in cases in which similar arguments are valid, and same results are obtained. In order to simplify the notation we define $\beta = \sqrt{c_3^2 + 4c_2(a_0 - 2c_0)}$.

• If $c_3^2 < -4c_2(a_0 - 2c_0)$ and $c_2c_3 > 0$, then P is an unstable focus. The reasoning is analogous to the one of the previous case and we obtain the same phase portraits: (L11) if $c_2 > 0$, and (L8) if $c_2 < 0$.

• If $c_3^2 = -4c_2(a_0 - 2c_0)$ and $c_2c_3 < 0$ or if $c_3^2 > -4c_2(a_0 - 2c_0)$, $c_2(c_3 - \beta) < 0$ and $c_2(c_3 + \beta) < 0$, then P is a stable node. If $c_3^2 = -4c_2(a_0 - 2c_0)$ and $c_2c_3 > 0$ or if $c_3^2 > -4c_2(a_0 - 2c_0)$, $c_2(c_3 - \beta) > 0$ and $c_2(c_3 + \beta) > 0$, then P is an unstable node. In both cases the phase portrait obtained is again (L11) if $c_2 > 0$, and (L8) if $c_2 < 0$.

• If $c_3 = 0$ and $c_2(a_0 - 2c_0) < 0$ then P is a linear center. In this case the singular point P could be a center or a focus, but the final phase portrait obtained when P is a center is the same as the one we obtained previously for the case with a focus, so the result is (L11) if $c_2 > 0$, and (L8) if $c_2 < 0$.

• If $c_3^2 > -4c_2(a_0 - 2c_0)$ and $(c_3 - \beta)(c_3 + \beta) < 0$, or if $c_3 = 0$ and $c_2(a_0 - 2c_0) > 0$, then P is a saddle. The blowing-down considering $c_2 > 0$ is represented in Figure 7. The final result is (L17) of Figure 1. If we take $c_2 < 0$ we obtain the phase portrait (L18).

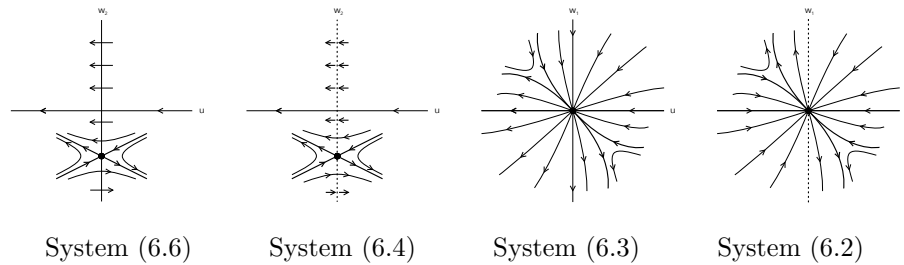


FIGURE 7. Desingularization of the origin of system (6.1) with $c_1 \neq 0$. Dicritical case (5), $c_2 > 0$.

6.2. Case c_1 zero. We consider system (6.1) and do the same variable change that we did in the case with $c_1 \neq 0$, the result is obviously system (6.2) but taking $c_1 = 0$, i.e.

$$\begin{aligned} \dot{u} &= (c_0 - a_0)u^3w_1^2 + c_3(\mu + 1)u^3w_1 + c_2(\mu + 1)u^3, \\ \dot{w}_1 &= -c_0u^2w_1^3 - c_3u^2w_1^2 - c_2u^2w_1. \end{aligned} \tag{6.7}$$

In this case we can cancel a common factor u^2 getting the system

$$\begin{aligned} \dot{u} &= (c_0 - a_0)uw_1^2 + c_3(\mu + 1)uw_1 + c_2(\mu + 1)u, \\ \dot{w}_1 &= -c_0w_1^3 - c_3w_1^2 - c_2w_1, \end{aligned} \tag{6.8}$$

for which we must study the singular points on the exceptional divisor, i.e. on the straight line $u = 0$.

The origin $S_0 = (0, 0)$ is always a singular point. The other singular points on this line are those for which w_1 is a solution of $c_0w_1^2 + c_3w_1 + c_2 = 0$. If $c_0 \neq 0$ and $c_3^2 > 4c_0c_2$ then $S_1 = (0, -(R_c + c_3)/(2c_0))$ and $S_2 = (0, (R_c - c_3)/(2c_0))$ are singular points. If $c_0 \neq 0$ and $c_3^2 = 4c_0c_2$, then $S_3 = (0, -c_3/2c_0)$ is a singular point, and finally, if c_0 and c_3 are non-zero, $S_4 = (0, -c_2/c_3)$ is a singular point.

TABLE 8. Cases with the singular points on the exceptional divisor of system (6.8).

Case	Conditions	Singular points
A	$c_0 = 0, c_3 = 0.$	$S_0.$
B	$c_0 = 0, c_3 \neq 0.$	$S_0, S_4.$
C	$c_0 \neq 0, c_3^2 < 4c_0c_2.$	$S_0.$
D	$c_0 \neq 0, c_3^2 = 4c_0c_2.$	$S_0, S_3.$
E	$c_0 \neq 0, c_3^2 > 4c_0c_2.$	$S_0, S_1, S_2.$

In summary we shall study the five cases given in Table 8. For doing this we study separately the local phase portrait of each singular point assuming in each case the necessary hypothesis for its existence.

The singular points S_0, S_1 and S_2 are hyperbolic. S_0 is a saddle if $\mu > -1$, a stable node if $c_2 > 0$ and $\mu < -1$, and an unstable node if $c_2 < 0$ and $\mu < -1$. S_1 is a saddle if $c_0(a_0 + c_0\mu) < 0$, a stable node if $c_0 > 0$ and $(a_0 + c_0\mu) > 0$, and an unstable node if $c_0 < 0$ and $(a_0 + c_0\mu) < 0$. S_2 is a saddle if $c_0(a_0 + c_0\mu)(R_c - c_3) < 0$, a stable node if $c_0(R_c - c_3) > 0$ and $(a_0 + c_0\mu) > 0$, and an unstable node if $c_0(R_c - c_3) < 0$ and $(a_0 + c_0\mu) < 0$.

The singular point S_3 is a semi-hyperbolic saddle-node and finally, S_4 is a hyperbolic saddle if $c_2 > 0$, and a hyperbolic stable node if $c_2 < 0$.

Using these informations we study the next cases from the five given in Table 8.

First of all we study case (A) in which the only singular point is the origin, so we have the next three possibilities.

If $c_0 = c_3 = 0$ and $\mu > -1$, then S_0 is a saddle. To determine the phase portrait around the w_1 -axis for system 6.8, we must fix the sign of c_2 , which determines the sense of the flow along the axes. Considering $c_2 > 0$ we obtain the phase portrait given in Figure (1)(L19), and with $c_2 < 0$ we obtain the phase portrait (L20).

If $c_0 = c_3 = 0$, $\mu < -1$ and $c_2 > 0$, then S_0 is a stable node, and we obtain the phase portrait (L21) of Figure (1).

If $c_0 = c_3 = 0$, $\mu < -1$ and $c_2 < 0$, then S_0 is an unstable node, and we obtain the phase portrait (L22) of Figure (1).

In case (B), fixed the phase portrait of S_4 , only two phase portraits will be possible for the origin, as the sign of c_2 is determined, and so we obtain the four following cases.

If $c_0 = 0, c_3 \neq 0, \mu > -1$ and $c_2 > 0$, then S_0 and S_4 are both saddle points and from the blowing-down we obtain the phase portrait (L23) of Figure (1).

If $c_0 = 0, c_3 \neq 0, \mu > -1$ and $c_2 < 0$, then S_0 is a saddle and S_4 a stable node. We obtain the phase portrait (L24) of Figure (1).

If $c_0 = 0, c_3 \neq 0, \mu < -1$ and $c_2 > 0$, then S_0 is a stable node and S_4 a saddle. We obtain the phase portrait (L25) of Figure (1).

If $c_0 = 0, c_3 \neq 0, \mu < -1$ and $c_2 < 0$, then S_0 is an unstable node and S_4 a stable node. We obtain the phase portrait (L26) of Figure (1).

Again in case (C) the only singular point is the origin so we distinguish three cases, and obtain the same local phase portrait that in case (A), but under different conditions. If $c_0 \neq 0, c_3^2 < 4c_0c_2$ and $\mu > -1$, then S_0 is a saddle. Attending to

the sign of c_2 , which determines the sense of the flow on the axes, we consider the following cases: if $c_2 > 0$ we obtain the phase portrait (L19) of Figure (1), and if $c_2 < 0$ we obtain the phase portrait (L20) of Figure (1).

If $c_0 \neq 0$, $c_3^2 < 4c_0c_2$, $\mu < -1$ and $c_2 > 0$, then S_0 is a stable node. We obtain the phase portrait (L21) of Figure (1).

If $c_0 \neq 0$, $c_3^2 < 4c_0c_2$, $\mu < -1$ and $c_2 < 0$, then S_0 is an unstable node. We obtain the phase portrait (L22) of Figure (1).

In case (D) apart from the origin, there exists the singular point S_3 , which is always a saddle node, so again we obtain only three cases.

If $c_0 \neq 0$, $c_3^2 = 4c_0c_2$ and $\mu > -1$, then S_0 is a saddle and S_3 a saddle-node. We must distinguish four subcases according to the signs of c_0 and $a_0 + c_0\mu$, which determine the position of the saddle-node S_3 and its sectors.

If $c_0 > 0$ and $a_0 + c_0\mu > 0$ we obtain the phase portrait (L27) of Figure (1), if $c_0 > 0$ and $a_0 + c_0\mu < 0$ we obtain the phase portrait (L28) of Figure (1), if $c_0 < 0$ and $a_0 + c_0\mu > 0$ we have the phase portrait (L29), and if $c_0 < 0$ and $a_0 + c_0\mu < 0$ the phase portrait (L30).

If $c_0 \neq 0$, $c_3^2 = 4c_0c_2$, $\mu < -1$ and $c_2 > 0$, then S_0 is a stable node and S_3 a saddle-node. We distinguish two subcases setting the sign of $a_0 + c_0\mu$ which determines the position of the sectors of the saddle-node S_3 . If $a_0 + c_0\mu > 0$ we obtain the phase portrait (L31) of Figure (1), and if $a_0 + c_0\mu < 0$ we obtain the phase portrait (L32) of Figure (1).

If $c_0 \neq 0$, $c_3^2 = 4c_0c_2$, $\mu < -1$ and $c_2 < 0$, then S_0 is an unstable node and S_3 a saddle-node. The only possibility is that $a_0 + c_0\mu > 0$, and we obtain the phase portrait (L33) of Figure (1).

In case (E) there exist three singular points, with three possible phase portraits for each of them, however, many of the combinations are not possible, and only 13 cases will be feasible.

First, due to the conditions which define the local phase portrait in each singular point, it is obvious that if S_1 is a stable node, then S_2 cannot be an unstable node, and if S_1 is an unstable node, S_2 cannot be a stable node, due to the sign of $a_0 + c_0\mu$.

If S_0 and S_2 were stable nodes and S_1 a saddle, the conditions $c_2 > 0$, $R_c - c_3 < 0$, and $c_0 < 0$ will hold. Squaring both terms in the condition $R_c < c_3$ we obtain $c_3^2 - 4c_0c_2 < c_3^2$, and then $c_0c_2 > 0$, which is a contradiction. The same reasoning is valid in the next two cases.

If S_0 and S_2 are unstable nodes and S_1 a saddle, then the conditions $c_2 < 0$, $R_c - c_3 < 0$ and $c_0 > 0$ hold, and if S_0 is an unstable node, S_1 a stable node and S_2 a saddle, then the same three conditions hold.

If S_0 , S_1 and S_2 are stable nodes, the conditions $c_2 > 0$, $R_c - c_3 > 0$ and $c_0 > 0$ hold. Now we take condition $R_c < c_3$ and squaring both terms we obtain $c_3^2 - 4c_0c_2 < c_3^2$, and then $c_0c_2 > 0$, which is a contradiction.

If S_0 is a stable node and S_1 an unstable node, the conditions $\mu < -1$, $c_0 < 0$ and $a_0 + c_0\mu < 0$ hold. Then according to the signs of c_0 and μ which are fixed, $a_0 < -c_0\mu < 0$ which contradicts the hypothesis (H1). The same reasoning is valid if S_0 and S_1 are unstable nodes, because the same conditions hold. Now we will study the feasible cases.

(E1) If $c_0 \neq 0$, $c_3^2 > 4c_0c_2$, $\mu > -1$, $c_0(a_0 + c_0\mu)(2c_0c_2 - c_3^2 - c_3R_c) > 0$ and $c_0(a_0 + c_0\mu)(R_c - c_3)(2c_0c_2 - c_3^2 + c_3R_c) > 0$, then S_0 , S_1 and S_2 are saddles. We must distinguish two subcases depending on the position of the singular points S_1

and S_2 on the w_1 -axis. First if S_1 is on the negative w_1 -axis and S_2 on the positive w_1 -axis, that corresponds with conditions $c_0 > 0$, $R_c - c_3 > 0$ and $c_2 < 0$, we obtain the phase portrait (L34) of Figure 1. Note that if $R_c - c_3 > 0$, the singular points S_1 and S_2 are one on the positive part of the axis and the other on the negative part, but in any case the absolute value of the second coordinate of S_1 is greater or equal than the absolute value of the second coordinate of S_2 , and this determines the relation between the slopes of orbits in the phase portraits. Conversely if we have S_1 on the positive w_1 -axis and S_2 on the negative one, i.e. under the conditions $c_0 < 0$, $R_c - c_3 > 0$ and $c_2 > 0$, we obtain the phase portrait (L35) of Figure (1).

(E2) If $c_0 \neq 0$, $c_3^2 > 4c_0c_2$, $\mu > -1$, $c_0(a_0 + c_0\mu)(2c_0c_2 - c_3^2 - c_3R_c) > 0$, $c_0(R_c - c_3) > 0$ and $(a_0 + c_0\mu)(2c_0c_2 - c_3^2 + c_3R_c) < 0$, then S_0 and S_1 are saddles and S_2 is a stable node. If $c_0 > 0$ then $R_c - c_3 > 0$ and so $c_3^2 - 4c_0c_2 > c_3^2$ and $c_0c_2 < 0$. If $a_0 + c_0\mu > 0$ then $2c_0c_2 - c_3^2 - c_3R_c > 0$ which is not possible because $2c_0c_2 < 0$ and we subtract two positive terms. Conversely if $a_0 + c_0\mu < 0$ then $2c_0c_2 - c_3^2 < c_3R_c$ and $2c_0c_2 - c_3^2 > -c_3R_c$, so $|2c_0c_2 - c_3^2| < c_3R_c$. Squaring we obtain $4c_0^2c_2^2 < 0$ which is not possible. If $c_0 < 0$ then $R_c - c_3 < 0$ and we deduce $c_2 < 0$. If $a_0 + c_0\mu < 0$ then $2c_0c_2 - c_3^2 - c_3R_c > 0$, but $c_3^2 - 2c_0c_2 > c_3^2 - 4c_0c_2 > 0$ so $2c_0c_2 - c_3^2 < 0$ and subtracting $c_3R_c > 0$ the result cannot be positive. In conclusion we deduce that $c_0, c_2 < 0$ and $a_0 + c_0\mu > 0$. Hence we have $-(R_c + c_3)/(2c_0) > (R_c - c_3)/(2c_0) > 0$. This determines the only possible position of the singular points which are both in the positive w_1 -axis. Undoing the blow up we obtain the phase portrait (L36) of Figure 1.

(E3) If $c_0 \neq 0$, $c_3^2 > 4c_0c_2$, $\mu > -1$, $c_0(a_0 + c_0\mu)(2c_0c_2 - c_3^2 - c_3R_c) > 0$, $c_0(R_c - c_3) < 0$ and $(a_0 + c_0\mu)(2c_0c_2 - c_3^2 + c_3R_c) > 0$, then S_0 and S_1 are saddles and S_2 is an unstable node. Therefore we deduce that $0 > (R_c - c_3)/(2c_0) > -(R_c + c_3)/(2c_0)$, so both singular points are on the negative w_1 axis, S_1 under S_2 . We obtain the phase portrait (L37) of Figure (1).

(E4) If $c_0 \neq 0$, $c_3^2 > 4c_0c_2$, $\mu > -1$, $c_0 > 0$, $(a_0 + c_0\mu)(2c_0c_2 - c_3^2 - c_3R_c) < 0$ and $c_0(R_c - c_3)(a_0 + c_0\mu)(2c_0c_2 - c_3^2 + c_3R_c) > 0$, then S_0 and S_2 are saddles and S_1 is a stable node. Then we deduce that $-(R_c + c_3)/(2c_0) < (R_c - c_3)/(c_0) < 0$, so both singular points are on the negative w_1 axis, S_1 under S_2 . We obtain the phase portrait (L38) of Figure (1).

(E5) If $c_0 \neq 0$, $c_3^2 > 4c_0c_2$, $\mu > -1$, $c_0 > 0$, $(a_0 + c_0\mu)(2c_0c_2 - c_3^2 - c_3R_c) < 0$, $c_0(R_c - c_3) > 0$ and $(a_0 + c_0\mu)(2c_0c_2 - c_3^2 + c_3R_c) < 0$, then S_0 is a saddle and S_1 and S_2 are stable nodes. We obtain the phase portrait (L45) of Figure (1).

(E6) If $c_0 \neq 0$, $c_3^2 > 4c_0c_2$, $\mu > -1$, $c_0 < 0$, $(a_0 + c_0\mu)(2c_0c_2 - c_3^2 - c_3R_c) > 0$ and $(a_0 + c_0\mu)(R_c - c_3)(2c_0c_2 - c_3^2 + c_3R_c) < 0$, then S_0 and S_2 are saddles and S_1 is an unstable node. Hence we deduce that $0 < (R_c - c_3)/(2c_0) < -(R_c + c_3)/(2c_0)$, so both singular points are on the positive w_1 axis, S_2 under S_1 . We obtain the phase portrait (L47) of Figure (1).

(E7) If $c_0 \neq 0$, $c_3^2 > 4c_0c_2$, $\mu > -1$, $c_0 < 0$, $(a_0 + c_0\mu)(2c_0c_2 - c_3^2 - c_3R_c) > 0$, $R_c - c_3 > 0$ and $(a_0 + c_0\mu)(2c_0c_2 - c_3^2 + c_3R_c) > 0$, then S_0 is a saddle and S_1 and S_2 are unstable nodes. We obtain the phase portrait (L46) of Figure (1).

(E8) If $c_0 \neq 0$, $c_3^2 > 4c_0c_2$, $c_2 > 0$, $\mu < -1$, $c_0(a_0 + c_0\mu)(2c_0c_2 - c_3^2 - c_3R_c) > 0$ and $c_0(a_0 + c_0\mu)(R_c - c_3)(2c_0c_2 - c_3^2 + c_3R_c) > 0$, then S_0 is a stable node and S_1 and S_2 are saddles. We obtain the phase portrait (L39) of Figure (1).

(E9) If $c_0 \neq 0$, $c_3^2 > 4c_0c_2$, $c_2 > 0$, $\mu < -1$, $c_0(a_0 + c_0\mu)(2c_0c_2 - c_3^2 - c_3R_c) > 0$, $c_0(R_c - c_3) < 0$ and $(a_0 + c_0\mu)(2c_0c_2 - c_3^2 + c_3R_c) > 0$, then S_0 is a stable node,

S_1 is a saddle and S_2 is an unstable node. We obtain the phase portrait (L40) of Figure (1).

(E10) If $c_0 \neq 0$, $c_3^2 > 4c_0c_2$, $c_2 > 0$, $\mu < -1$, $c_0 > 0$, $(a_0 + c_0\mu)(2c_0c_2 - c_3^2 - c_3R_c) < 0$ and $(a_0 + c_0\mu)(R_c - c_3)(2c_0c_2 - c_3^2 + c_3R_c) > 0$, then S_0 and S_1 are stable nodes and S_2 is a saddle. We obtain the phase portrait (L41) of Figure (1).

(E11) If $c_0 \neq 0$, $c_3^2 > 4c_0c_2$, $c_2 < 0$, $\mu < -1$, $c_0(a_0 + c_0\mu)(2c_0c_2 - c_3^2 - c_3R_c) > 0$, and $c_0(a_0 + c_0\mu)(R_c - c_3)(2c_0c_2 - c_3^2 + c_3R_c) > 0$, then S_0 is an unstable node and S_1 and S_2 are saddles. We obtain the phase portrait (L42) of Figure (1).

(E12) If $c_0 \neq 0$, $c_3^2 > 4c_0c_2$, $c_2 < 0$, $\mu < -1$, $c_0(a_0 + c_0\mu)(2c_0c_2 - c_3^2 - c_3R_c) > 0$, $c_0(R_c - c_3) > 0$, and $(a_0 + c_0\mu)(2c_0c_2 - c_3^2 + c_3R_c) < 0$, then S_0 is an unstable node, S_1 is a saddle and S_2 is a stable node. We obtain the phase portrait (L43) of Figure (1).

(E13) If $c_0 \neq 0$, $c_3^2 > 4c_0c_2$, $c_2 < 0$, $\mu < -1$, $c_0 > 0$, $(a_0 + c_0\mu)(2c_0c_2 - c_3^2 - c_3R_c) < 0$, $R_c - c_3 > 0$, and $(a_0 + c_0\mu)(2c_0c_2 - c_3^2 + c_3R_c) < 0$, then S_0 is an unstable node and S_1 and S_2 are stable nodes. We obtain the phase portrait (L44) of Figure (1).

Note that in the phase portraits (L22), (L30), (L33), (L43), (L46) and (L47) of Figure 1 it is possible to consider hyperbolic sectors instead of the elliptic ones, but we have only represented the elliptic cases by the same reason given before, i.e. because applying the index theory to the phase portraits in the sphere \mathbb{S}^2 described in Section 7, we proved that they are the only feasible.

Once we completed the study in the local chart U_1 , we study the origin of chart U_2 which turned out to be much simpler. The system has the expression

$$\begin{aligned} \dot{u} &= -c_1(\mu + 1)u^2v + (a_0 - c_0)uv^2 - c_3(\mu + 1)uv - c_2(\mu + 1)u, \\ \dot{v} &= -c_1uv^2 - c_0v^3 - c_3v^2 - c_2v. \end{aligned} \quad (6.9)$$

Lemma 6.2. *The origin of chart U_2 is always a hyperbolic infinite singular point of system (1.3). It is a saddle if $\mu < -1$, a stable node if $c_2 > 0$ and $\mu > -1$, and an unstable node if $c_2 < 0$ and $\mu > -1$.*

7. GLOBAL PHASE PORTRAITS

To prove the global result stated in Theorem 1.1, we will bring together the local information obtained in the previous sections. We start our classification from the cases in Tables 2 to 7. In some of them the conditions determine only one local phase portrait in each one of the infinite singular points but, in many others we shall distinguish several possibilities. In some cases the local information gives rise to only one phase portrait, this occurs when the separatrices can be connected in only one way, but in others several global possibilities appear, and we shall prove which of them are feasible.

In Table 9 we give, for each case in the Tables 2 to 7, the local phase portrait of the infinite singularities O_1 and O_2 (in most cases this depends on the parameters), and also we give the global phase portrait on the Poincaré disc obtained. And now we detail the reasonings in some cases, although they will not be showed in all cases to avoid repetitions.

Case 1.1. The infinite singular point O_1 has the local phase portrait (L12) given in Figure 1, and O_2 is an unstable node. As we said in Section 6, the elliptic sectors appearing in phase portrait (L12) could be hyperbolic sectors if we attend only to local results, but now having all the global information we can prove that they are elliptic by using the index theory. By Theorem 2.2 the sum of the indices of all

the singular points on the Poincaré sphere has to be 2. To compute this sum we must consider that the finite singular points on the Poincaré disc appear twice on the sphere (on the northern hemisphere and on the southern hemisphere). Thus if we denote by ind_F the sum of the indices of the finite singular points, and by ind_I the sum of the indices of the infinite singular points, the equality $2 \text{ind}_F + \text{ind}_I = 2$ must be satisfied.

In this particular case the finite singular points are a saddle-node whose index is 0, and two saddles whose index is -1 , so $\text{ind}_F = -2$. We deduce that ind_I must be 6. The infinite singular points are O_1 and O_2 , the origins of the local charts U_1 and U_2 , and the origins of the symmetric local charts V_1 and V_2 , which have the same index. Since O_2 is a node, and so it has index 1, we obtain that the sum of the indices of O_2 and its symmetric must be 4, i.e. the index of O_2 has to be 2. From the Poincaré formula for the index given in subsection 2.4 we obtain

$$\frac{e - h}{2} + 1 = 2 \implies e - h = 2.$$

Hence only the case with two elliptic sectors on the local phase portrait (L12) is possible, because if we had two hyperbolic sectors instead of the elliptic ones, the index of O_2 would be zero.

We recall that by an analogous application of the index theory in the corresponding cases, it can be concluded that elliptic sectors appearing in the local phase portraits (L8), (L9), (L11), (L22), (L30), (L33), (L43), (L46) and (L47) of O_1 , are indeed elliptic rather than hyperbolic.

In this case 1.1 there is only one possible phase portrait on the Poincaré disc, the one given in Figure (16) (G1).

Case 1.6. In this case O_1 has the local phase portrait (L3) and O_2 is a stable node. From the local results we can obtain three possible global phase portraits given in Figure 8.

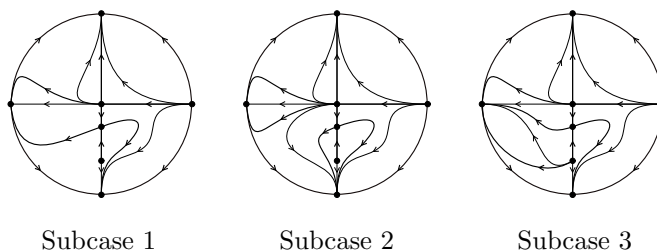


FIGURE 8. Possible global phase portraits in case 1.6.

By Theorem 4.8 on the straight lines $z = z_0 \neq 0$ cannot be more than one contact point, but as it is shown in Figure 9, if subcases 1 and 2 are feasible, there exist straight lines $z = z_0$, with $-(R_c + c_3)/(2c_2) < z_0 < (R_c - c_3)/(2c_2)$, on which there exist two contact points, so we deduce that the only possible global phase portrait is the subcase 3, i.e. (G10) of Figure 16.

Case 1.10. In this case O_1 has the local phase portrait (L6) and O_2 is an unstable node. From the local results we can obtain three possible global phase portraits, but in two of them shown in Figure 10 we can find straight lines $z = z_0 \neq 0$ with $(R_c - c_3)/(2c_2) < z_0 < -(R_c + c_3)/(2c_2)$, on which there are two contact points,

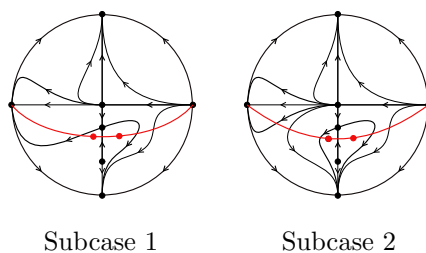


FIGURE 9. Straight lines with two contact points on the two first subcases of 1.6

so according to Theorem 4.8 they are not possible. Then the only possibility is the phase portrait (G20) of Figure 16.

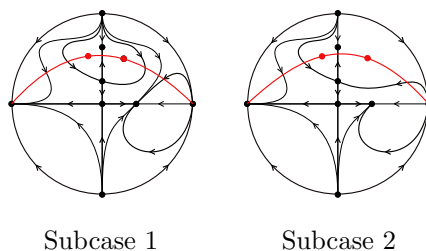


FIGURE 10. Straight lines with two contact points on two subcases of 1.10.

Case 2.2. In this case O_1 has the local phase portrait (L47) and O_2 is an unstable node. From the local results and by Theorem 4.3 the phase portrait is symmetric, we obtain three possible global phase portraits, the ones given of Figure 11.

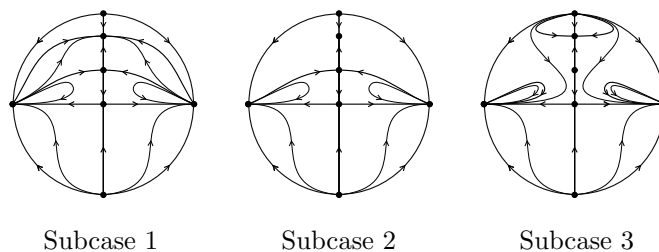


FIGURE 11. Possible global phase portraits in case (2.2).

By Theorem 4.8 we know that, under the conditions of this case, two invariant straight lines $z = \pm(R_c - c_3)/(2c_2)$ must exist, and it is only possible in the subcase 1, which provides the phase portrait (G42) of Figure 16.

Case 2.6. Here we distinguish three subcases and, in two of them, three global phase portraits appear, but in each case we use different arguments to prove which of the options is realizable. If $\mu = 0$, then O_1 has the local phase portrait (L5) and

O_2 is a stable node. We obtain three phase portraits, but we conclude that two of them are not feasible because we can find straight lines $z = z_0 \neq 0$ with two contact points, as it is shown in Figure 12. Therefore there is only one global phase portrait, the (G50) of Figure 16.

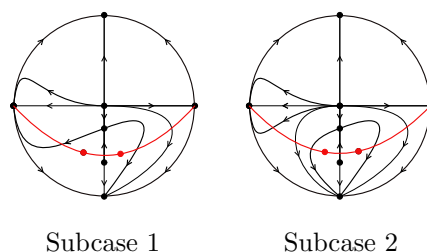


FIGURE 12. Straight lines with two contact points on two subcases.

If $c_1 = 0$ and $\mu > -1$, then O_1 has the local phase portrait (L38) and O_2 is a stable node. We obtain three possible global phase portraits, the ones given in Figure 13. By Theorem 4.8 we know that, under the conditions of this case, two invariant straight lines $z = \pm(R_c - c_3)/(2c_2)$ must exist, and it is only possible in the subcase 3, which provides the phase portrait (G51) of Figure 16.

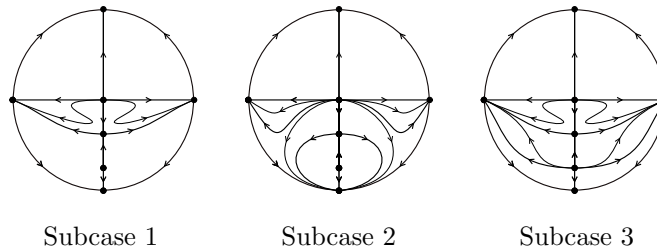


FIGURE 13. Possible global phase portraits in case 2.6 with $c_1 = 0$ and $\mu > -1$.

If $c_1 = 0$ and $\mu < -1$, then O_1 has the local phase portrait (L41) and O_2 is a saddle. In this case we obtain only one phase portrait (G52) of Figure 16.

Case 3.2. Here we distinguish three subcases and in two of them there is only one possible global phase portrait. More precisely, if $\mu < -1$ then O_1 has the local phase portrait (L8), O_2 is a saddle and the global phase portrait is (G64). If $\mu \in (-1, 0)$ then O_1 has the local phase portrait (L13), O_2 is an unstable node and we obtain the phase portrait (G65).

If $\mu > 0$ then O_1 has the local phase portrait (L6) and O_2 is an unstable node, but in this case we obtain three phase portraits, the ones given in Figure 14. By Theorem 4.8, there must exist a contact point on each straight line $z = z_0$, but if in subcases 1 and 2 we take a straight line $z = z_0$ with $z_0 > -c_3/(2c_2)$, there are not contact points on it, so those subcases are not feasible. The only possibility is the subcase 3, which provides the phase portrait (G63) of Figure 16.

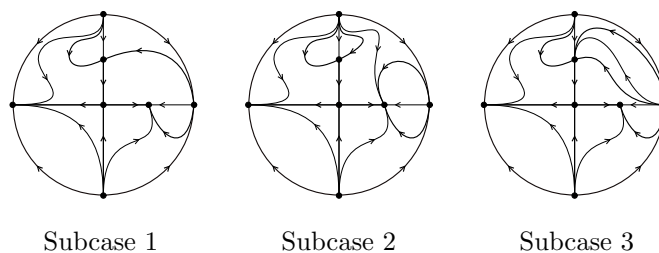


FIGURE 14. Possible global phase portraits in case 3.2 with $\mu > 0$.

Case 4.2. Here we distinguish five different subcases. First if $c_1 = 0$, $\mu < -1$ and $a_0 + c_0\mu > 0$, then O_1 has the local phase portrait (L31) and O_2 is a saddle. In this case we obtain the global phase portrait (G90).

If $c_1 = 0$, $\mu < -1$ and $a_0 + c_0\mu < 0$, then O_1 has the local phase portrait (L32) and O_2 is a saddle. By Corollary 4.3 the phase portrait must be symmetric so we obtain three possibilities, given in Figure 15. We further know that there must exist an invariant straight line $z = -c_3/2c_2$, so we can deduce that subcase 2 is not feasible because that invariant straight line does not exist. As we also know that this invariant straight line is a separatrix in the local phase portrait of O_1 , the one appearing in (L32), the subcase 3 is not feasible, because there would exist another separatrix over the invariant straight line that does not appear on (L32). So finally the only possible phase portrait is (G91).

The same happens in the next cases in which we initially obtain three possibilities but we can discard two of them with the same arguments, so finally we obtain the next results. If $\mu = 0$, then O_1 has the local phase portrait (L5) and O_2 is a stable node and we obtain the global phase portrait (G87). If $c_1 = 0$, $\mu > -1$ and $a_0 + c_0\mu > 0$, then O_1 has the local phase portrait (L27), O_2 is a stable node, and we obtain the phase portrait (G88). Finally if $c_1 = 0$, $\mu > -1$ and $a_0 + c_0\mu < 0$, then O_1 has the local phase portrait (L28), O_2 is a stable node, and the global phase portrait is (G89).

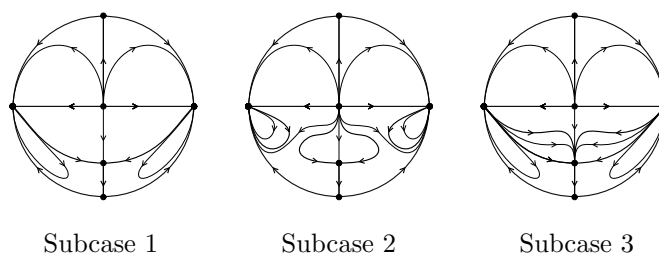


FIGURE 15. Possible global phase portraits in case 4.2 with $c_1 = 0$, $\mu < -1$ and $a_0 + c_0\mu < 0$.

The same methods that we have used in the previous cases for determine which of the global phase portraits are realizable, must be used in some other cases, namely, 1.17, 1.18 with $\mu \geq -2$, 1.19, 2.7, 3.3, 3.4 with $\mu \geq -2$, 3.5 with $\mu > 0$, and finally 4.1 with $c_1 = 0$, $\mu > -1$ and $a_0 + c_0\mu < 0$.

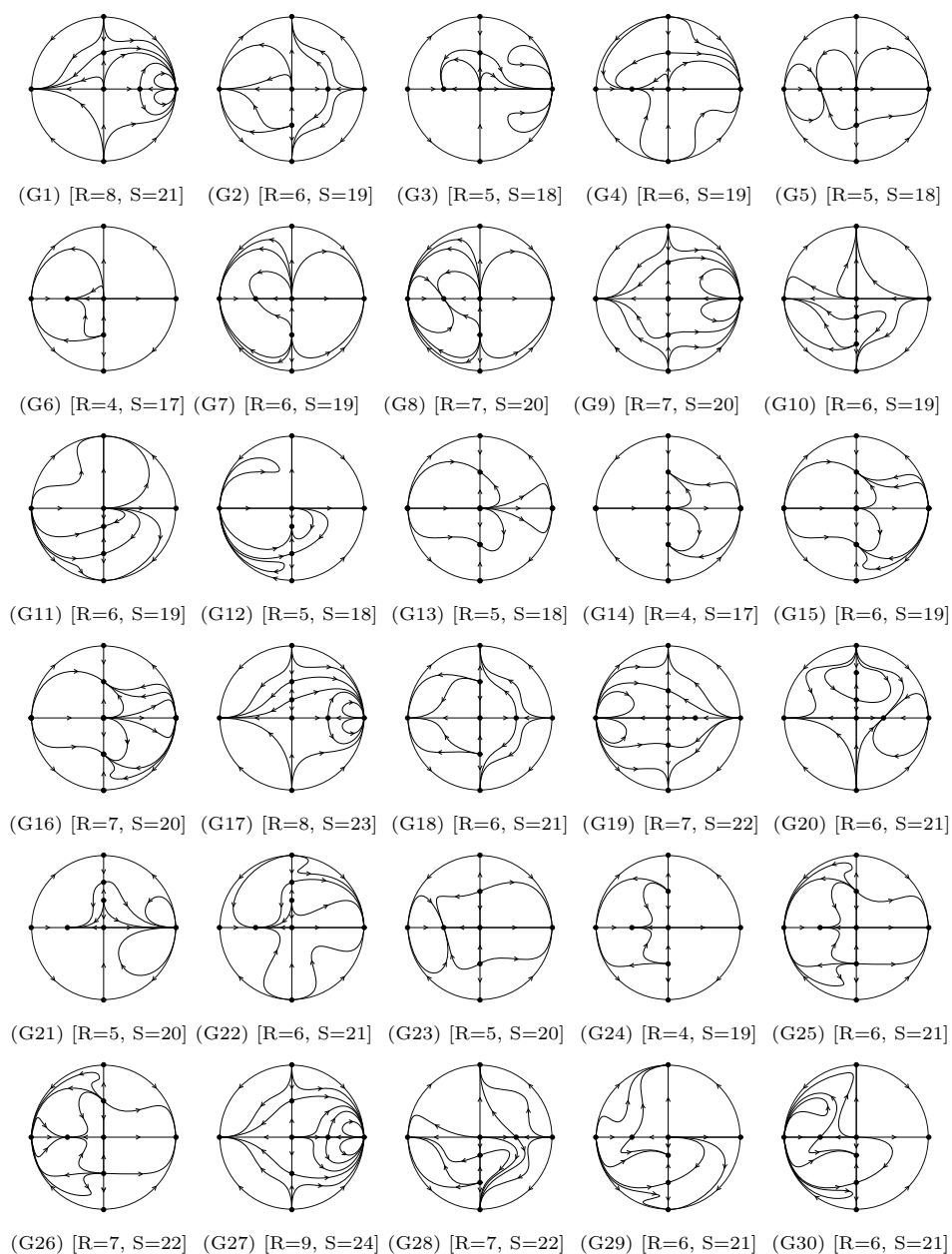


FIGURE 16. Global phase portraits of system (1.3) in the Poincaré disc (to be continued).

Remark 7.1. Global phase portraits (G43), (G48), (G57), (G84) and (G92) can appear both under condition $c_1 = 0$ or under $c_1 \neq 0$ so, as we are interested in the topological classification we represent only the non-symmetric case respect to z -axis, but also the symmetric is possible. The same situation occurs with

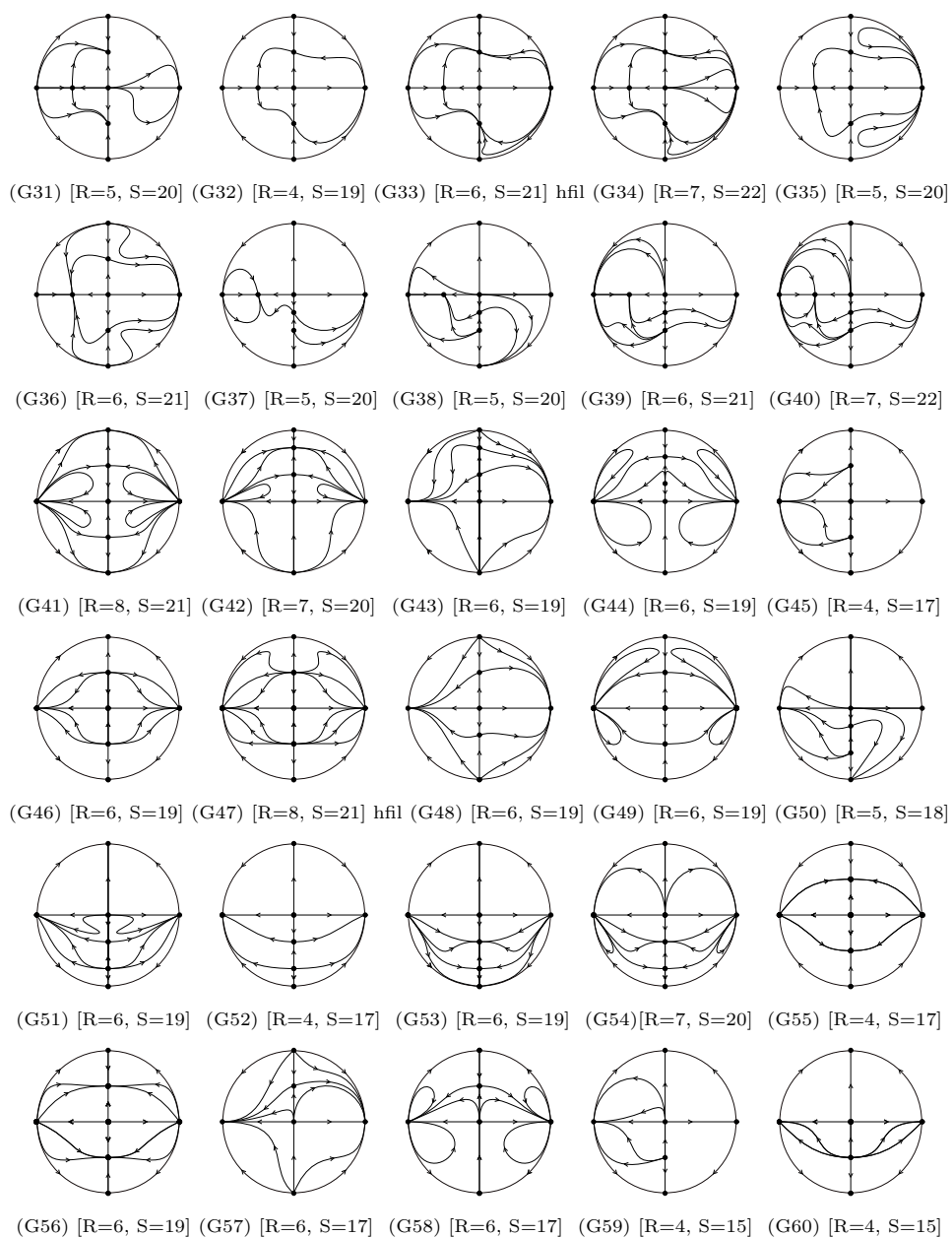


FIGURE 16. (cont.) Global phase portraits of system (1.3) in the Poincaré disc (to be continued).

the global phase portraits (G9), (G13)–(G16), (G18), (G19), (G23)–(G27), (G31)–(G36), (G41), (G45)–(G49), (G55), (G56), (G76)–(G83), (G92)–(G102), which can appear under the condition $c_3 = 0$ or $c_3 \neq 0$ so they can present the symmetric or the non-symmetric form respect to x -axis, although we only represent one of them because we are only interested on the topological classification.

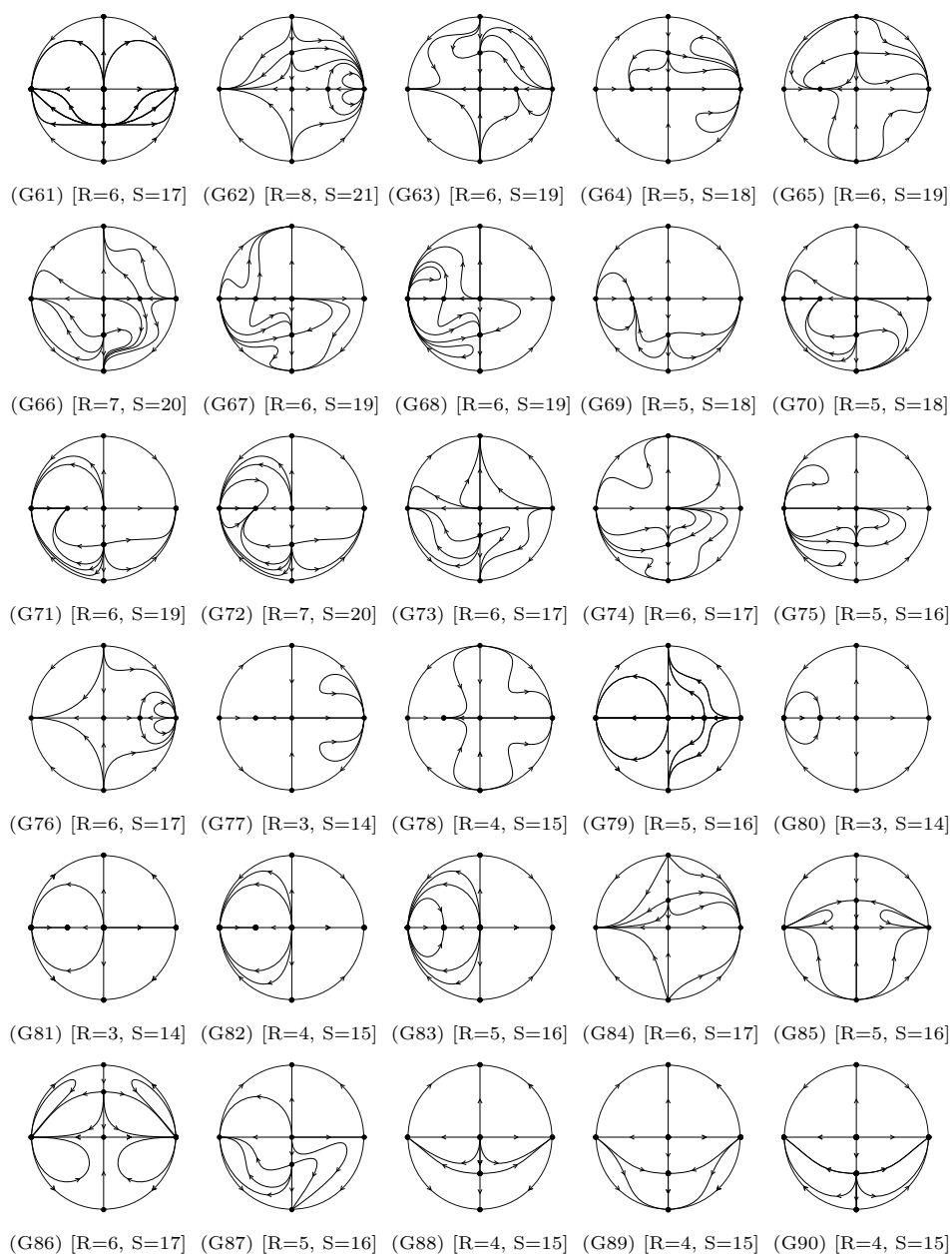


FIGURE 16. (cont.) Global phase portraits of system (1.3) in the Poincaré disc (to be continued).

Acknowledgements. E. Diz-Pita and M. V. Otero-Espinar were partially supported by the Ministerio de Economía, Industria y Competitividad, Agencia Estatal de Investigación (Spain), grant MTM2016-79661-P (European FEDER support included, UE) and the Consellería de Educación, Universidade e Formación Profesional (Xunta de Galicia), grant ED431C 2019/10 with FEDER funds. E.

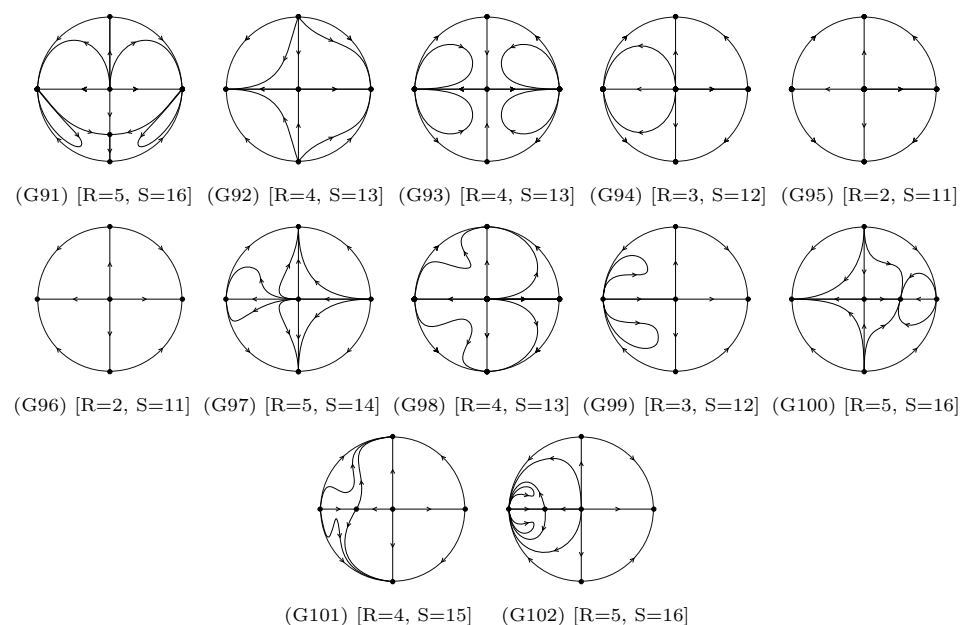


FIGURE 16. (cont.) Global phase portraits of system (1.3) in the Poincaré disc.

Diz-Pita was also supported by the Ministerio de Educacion, Cultura y Deporte de España, contract FPU17/02125.

J. Llibre was partially supported by the Ministerio de Ciencia, Innovación y Universidades, Agencia Estatal de Investigación grants MTM2016-77278-P (FEDER), the Agència de Gestió d'Ajuts Universitaris i de Recerca grant 2017SGR1617, and the H2020 European Research Council grant MSCA-RISE-2017-777911.

REFERENCES

- [1] J. Alavez-Ramírez, G. Blé, V. Castellanos, J. Llibre; On the global flow of a 3-dimensional Lotka-Volterra system, *Nonlinear Anal. Theor.*, **75** (2012), 4114-4125.
- [2] M. J. Alvarez, A. Ferragut, X. Jarque; A survey on the blow up technique, *Int. J. Bifurcat. Chaos.*, **21** (2011), 3103-3118.
- [3] A. A. Andronov, E. A. Leontovich, I.J. Gordon, A. G. Maier; *Qualitative Theory of 2nd Order Dynamic Systems*, J. Wiley & Sons, 1973.
- [4] R. Benterki, J. Llibre; Phase portraits of quadratic polynomial differential systems having as solution some classical planar algebraic curves of degree 4, *Electron. J. Differ. Eq.*, **2019** (2019), No. 15, 1-25.
- [5] P. Breitenlohner, G. Lavrelashvili, D. Maison; Mass inflation and chaotic behaviour inside hairy black holes, *Nucl. Phys. B*, **524** (1998), 427-443.
- [6] F.H. Busse; Transition to turbulence via the statistical limit cycle route, *Synergetics*, **39**, Springer-Verlag, Berlin, 1978.
- [7] M. Desai, P. Ormerod; Richard Goodwin: A Short Appreciation, *Econ. J.*, **108** (1998) No. 450, 1431-1435.
- [8] F. Dumortier; Singularities of vector fields on the plane; *J. Diff. Eq.*, **23** (1977), 53-106.
- [9] F. Dumortier, J. Llibre, J.C. Artés; *Qualitative Theory of Planar Differential Systems*, UniversiText, Springer-Verlag, New York, 2006.
- [10] G. Gandolfo; *Economic dynamics*, Fourth edition. Springer, Heidelberg, 2009. xxviii+749 pp.

- [11] G. Gandolfo; Giuseppe Palomba and the Lotka-Volterra equations; *Rend. Lince. - Sci. Fis.*, **19** (2008) No. 4, 347-357.
- [12] R. M. Goodwin; *A Growth Cycle*, C.H. Socialism, Capitalism and Economic Growth, Cambridge University Press, 1967.
- [13] J. Jiménez, J. Llibre, J. C. Medrado; Crossing limit cycles for a class of piecewise linear differential centers separated by a conic, *Electron. J. Differ. Eq.*, **2020** (2020), No. 41, 1-36.
- [14] A. Kolmogorov; Sulla teoria di Volterra della lotta per l'esistenza, *Gi. Inst. Ital. Attuari*, **7** (1936), 74-80.
- [15] G. Laval, R. Pellat; Plasma Physics, *Proceedings of Summer School of Theoretical Physics*, (1975).
- [16] J. Llibre, X. Zhang; Darboux theory of integrability in \mathbb{C}^n taking into account the multiplicity, *J. Differ. Equations*, **246** (2009), 541-551.
- [17] J. Llibre, W. F. Pereira, C. Pessoa; Phase portraits of Bernoulli quadratic polynomial differential systems, *Electron. J. Differ. Eq.*, **2020** (2020), No. 48, 1-19.
- [18] J. Llibre, X. Zhang; Darboux theory of integrability for polynomial vector fields in \mathbb{R}^n taking into account the multiplicity at infinity, *B. Sci. Math.*, **133** (2009), 765-778.
- [19] J. Llibre, X. Zhang; Rational first integrals in the Darboux theory of integrability in \mathbb{C}^n , *B. Sci. Math.*, **134** (2010), 189-195.
- [20] R. M. May; *Stability and Complexity in Model Ecosystems*, Princeton NJ, 1974.
- [21] L. Markus; Global structure of ordinary differential equations in the plane, *Trans. Amer. Math. Soc.*, **76** (1954), 127-148.
- [22] D. A. Neumann; Classification of continuous flows on 2-manifolds, *Proc. Amer. Math. Soc.*, **48** (1975), 73-81.
- [23] M. M. Peixoto; *Proceedings of a simposium held at the university of Bahia*, Acad. Press, New York, 1973.
- [24] D. Schlomiuk, N. Vulpe; Global topological classification of Lotka-Volterra quadratic differential systems, *Electron. J. Differ. Eq.*, **2012** (2012), No. 64, 1-69.
- [25] A. W. Wijeratne, F. Yi, J. Wei; Bifurcation analysis in the diffusive Lotka-Volterra system: an application to market economy, *Chaos Soliton. Fract.*, **40** (2009), No. 2, 902-911.

ÉRIKA DIZ-PITA

DEPARTAMENTO DE ESTATÍSTICA, ANÁLISE MATEMÁTICA E OPTIMIZACIÓN, UNIVERSIDADE DE SANTIAGO DE COMPOSTELA, 15782 SANTIAGO DE COMPOSTELA, SPAIN

Email address: erikadiz.pita@usc.es

JAUME LLIBRE

DEPARTAMENT DE MATEMÀTIQUES, UNIVERSITAT AUTÒNOMA DE BARCELONA, 08193 BELLATERRA, BARCELONA, SPAIN

Email address: jllibre@mat.uab.cat

M. VICTORIA OTERO-ESPINAR

DEPARTAMENTO DE ESTATÍSTICA, ANÁLISE MATEMÁTICA E OPTIMIZACIÓN, UNIVERSIDADE DE SANTIAGO DE COMPOSTELA, 15782 SANTIAGO DE COMPOSTELA, SPAIN

Email address: mvictoria.otero@usc.es

TABLE 9. Classification of global phase portraits of system (1.3).

Case	Conditions	O_1	O_2	Global
1.1		L12	Unstable node	G1
1.2		L3	Stable node	G2
1.3	$\mu < -1$	L8	Saddle	G3
	$\mu \in (-1, 0)$	L13	Unstable node	G4
1.4	$\mu < -2$	L1	Saddle	G5
	$\mu \in (-1, 0)$	L4	Saddle	G7
	$\mu \in (-2, -1)$	L15	Saddle	G7
	$\mu = -2$	L17	Saddle	G8
1.5		L12	Unstable node	G9
1.6		L3	Stable node	G10
1.7	$\mu \in (-1, 0)$	L10	Stable node	G11
	$\mu < -1$	L11	Saddle	G12
1.8	$\mu < -2$	L2	Saddle	G13
	$\mu \in (-1, 0)$	L7	Unstable node	G14
	$\mu \in (-2, -1)$	L16	Saddle	G15
	$\mu = -2$	L18	Saddle	G16
1.9		L9	Stable node	G19
1.10		L6	Unstable node	G20
1.11		L12	Unstable node	G17
1.12	$\mu < -1$	L8	Saddle	G21
	$\mu \in (-1, 0)$	L13	Unstable node	G22
1.13		L3	Stable node	G18
1.14	$\mu < -2$	L1	Saddle	G23
	$\mu \in (-1, 0)$	L4	Stable node	G24
	$\mu \in (-2, -1)$	L15	Saddle	G25
	$\mu = -2$	L17	Saddle	G26
1.15		L12	Unstable node	G27
1.16	$\mu < -1$	L8	Saddle	G35
	$\mu \in (-1, 0)$	L13	Unstable node	G36
1.17		L3	Stable node	G28
1.18	$\mu < -2$	L1	Saddle	G37
	$\mu \in (-1, 0)$	L4	Stable node	G38
	$\mu \in (-2, -1)$	L15	Saddle	G39
	$\mu = -2$	L17	Saddle	G40
1.19	$\mu \in (-1, 0)$	L10	Saddle	G29
	$\mu < -1$	L11	Saddle	G30
1.20	$\mu < -2$	L2	Saddle	G31
	$\mu \in (-1, 0)$	L7	Unstable node	G32
	$\mu \in (-2, -1)$	L16	Saddle	G33
	$\mu = -2$	L18	Saddle	G34
2.1		L46	Stable node	G41
2.2		L47	Unstable node	G42
2.3	$\mu = 0$	L14	Unstable node	G43
	$c_1 = 0, \mu > -1$	L36		
	$c_1 = 0, \mu < -1$	L43	Saddle	G44

TABLE 9. (cont.) Classification of global phase portraits of system (1.3).

Case	Conditions	O_1	O_2	Global
2.4	$\mu = 0$	L5	Stable node	G45
	$c_1 = 0, \mu > -1$	L35	Stable node	G46
	$c_1 = 0, \mu < -1$	L39	Saddle	G47
2.5	$\mu = 0$	L14	Unstable node	G48
	$c_1 = 0, \mu > -1$	L45		
	$c_1 = 0, \mu < -1$	L44	Saddle	G49
2.6	$\mu = 0$	L5	Stable node	G50
	$c_1 = 0, \mu > -1$	L38	Stable node	G51
	$c_1 = 0, \mu < -1$	L41	Saddle	G52
2.7	$\mu > -1$	L37	Stable node	G53
	$\mu < -1$	L40	Saddle	G54
2.8	$\mu > -1$	L34	Unstable node	G55
	$\mu < -1$	L42	Saddle	G56
2.9	$\mu = 0$	L14	Unstable node	G57
	$c_1 = 0, \mu > -1$	L24		
	$c_1 = 0, \mu < -1$	L26	Saddle	G58
2.10	$\mu = 0$	L5	Stable node	G59
	$c_1 = 0, \mu > -1$	L23	Stable node	G60
	$c_1 = 0, \mu < -1$	L25	Saddle	G61
3.1		L12	Unstable node	G62
3.2	$\mu > 0$	L6	Unstable node	G63
	$\mu < -1$	L8	Stable node	G64
	$\mu \in (-1, 0)$	L13	Unstable node	G65
3.3	$\mu > 0$	L3	Stable node	G66
	$\mu < -1$	L11	Stable node	G68
	$\mu \in (-1, 0)$	L10	Stable node	G67
3.4	$\mu < -2$	L1	Saddle	G69
	$\mu \in (-1, 0)$	L4	Stable node	G70
	$\mu \in (-2, -1)$	L15	Saddle	G71
	$\mu = -2$	L17	Saddle	G72
3.5	$\mu > 0$	L3	Stable node	G7
	$\mu \in (-1, 0)$	L10	Stable node	G74
	$\mu < -1$	L11	Saddle	G75
3.6		L12	Unstable node	G76
3.7	$\mu < -1$	L8	Saddle	G77
	$\mu \in (-1, 0)$	L13	Unstable node	G78
3.8		L3	Stable node	G79
3.9	$\mu < -2$	L1	Saddle	G80
	$\mu \in (-1, 0)$	L4	Stable node	G81
	$\mu \in (-2, -1)$	L15	Saddle	G82
	$\mu = -2$	L17	Saddle	G83

TABLE 9. (cont.) Classification of global phase portraits of system (1.3).

Case	Conditions	O_1	O_2	Global
4.1	$\mu = 0$	L14	Unstable node	G84
	$c_1 = 0, \mu > -1, a_0 + c_0\mu > 0$	L29		
	$c_1 = 0, \mu > -1, a_0 + c_0\mu < 0$	L30	Unstable node	G85
	$c_1 = 0, \mu < -1$	L33	Saddle	G86
4.2	$\mu = 0$	L5	Stable node	G87
	$c_1 = 0, \mu > -1, a_0 + c_0\mu > 0$	L27	Stable node	G88
	$c_1 = 0, \mu > -1, a_0 + c_0\mu < 0$	L28	Stable node	G89
	$c_1 = 0, \mu < -1, a_0 + c_0\mu > 0$	L31	Saddle	G90
	$c_1 = 0, \mu < -1, a_0 + c_0\mu < 0$	L32	Saddle	G91
4.3	$\mu = 0$	L14	Unstable node	G92
	$c_1 = 0, \mu > -1$	L20		
	$c_1 = 0, \mu < -1$	L22	Saddle	G93
4.4	$\mu = 0$	L5	Stable node	G94
	$c_1 = 0, \mu > -1$	L19	Stable node	G95
	$c_1 = 0, \mu < -1$	L21	Saddle	G96
5.1	$\mu > 0$	L3	Stable node	G97
	$\mu \in (-1, 0)$	L10	Stable node	G98
	$\mu < -1$	L11	Saddle	G99
5.2		L12	Unstable node	G76
5.3	$\mu > 0$	L6	Unstable node	G100
	$\mu < -1$	L8	Saddle	G77
	$\mu \in (-1, 0)$	L13	Unstable node	G78
5.4	$\mu > 0$	L3	Stable node	G79
	$\mu \in (-1, 0)$	L10	Stable node	G101
	$\mu < -1$	L11	Saddle	G102
5.5	$\mu < -2$	L1	Saddle	G80
	$\mu \in (-1, 0)$	L4	Stable node	G81
	$\mu \in (-2, -1)$	L15	Saddle	G82
	$\mu = -2$	L17	Saddle	G83
6.1	$\mu = 0$	L14	Unstable node	G92
	$c_1 = 0, \mu > -1$	L20		
	$c_1 = 0, \mu < -1$	L22	Saddle	G93
6.2	$\mu = 0$	L5	Stable node	G94
	$c_1 = 0, \mu > -1$	L19	Stable node	G95
	$c_1 = 0, \mu < -1$	L21	Saddle	G96